CZECH TECHNICAL UNIVERSITY IN PRAGUE
FACULTY OF ELECTRICAL ENGINEERING
DEPARTMENT OF ELECTROMAGNETIC FIELD

Doctoral Thesis

Methodology of Magnetic Field Generation and Evaluation for Magnetic Particle Inspection

Ing. Pavel Staněk

Programme: Electrical Engineering and Information Technology (P2612)
Branch of study: Electrical Engineering Theory (2602V013)

Supervisor: prof. Ing. Zbyněk Škvor, CSc.

Prague, 2023

Declaration

I hereby declare I have written this thesis independently and have quoted all the sources of information used in accordance with the methodological instructions on ethical principles for writing an academic thesis. Moreover, I state that this thesis has neither been submitted nor accepted for any other degree.

January 2023, Prague

....

Pavel Staněk

Acknowledgement

Abstract

This thesis deals with material testing by magnetic particle inspection. The main objective is, with the help of theoretical analysis, to contribute to a better understanding of the physical mechanisms that apply in this process and to draw conclusions that can be directly used in practice in the design of test equipment. In particular, three topics are covered: magnetic field measurement, automated magnetic field evaluation and magnetic field generation.

Magnetic field measurement is an important mechanism for verifying the detection ability of magnetic particle inspection. In the thesis the common practice, based on the recommendations given by the standards, is discussed and the possibilities of how to make these procedures more efficient and faster by introducing vector measurement of the tangential magnetic field components are suggested.

Through the theoretical analysis of the physical mechanisms applied in the process of the formation of indications, a force impulse is introduced as a standard quantity for the evaluation of the generated magnetic field. The new method of evaluation of the magnetic field is based on vector measurement and the subsequent calculation of the force impulse on the detection particle. The proposed method also makes it possible to predict the influence of various factors on the quality of the indication. The ISO standard requires that magnetizing currents with a crest factor greater than three shall not be used without documented evidence of the effectiveness of the technique. However, the method of evaluation using impulse predicts a negligible effect of the crest factor of magnetizing currents on indication quality. The influence of the crest factor on the quality of the indications was experimentally investigated with results consistent with the impulse evaluation theory.

The last part of the thesis concerns magnetization methods for the detection of arbitrarily oriented defects. A method providing uniform detection capability in all directions using only a single-channel source of direct or alternating current is proposed. This magnetization method uses time-multiplexing between current loops and leads to a simplification of the test equipment design.

Abstrakt

Tato práce se zabývá materiálovým testováním magnetickou metodou práškovou. Hlavním cílem je za pomoci teoretického rozboru přispět k lepšímu porozumění fyzikálním mechanismům, které se uplatňují v tomto procesu a vyvodit závěry, které lze přímo využít v praxi při návrhu testovacích zařízení. Zejména jsou v práci řešena tři témata: měření magnetického pole, automatické vyhodnocování magnetického pole a generování magnetického pole.

Měření magnetického pole je jedním z důležitých mechanismů pro ověřování detekční schopnosti magnetické metody práškové. Proto je v práci diskutována běžná praxe vycházející z doporučení norem a dále je řešeno jak tyto postupy zefektivnit a zrychlit zavedením vektorového měření tečných složek magnetického pole.

Teoretickým rozborem fyzikálních mechanismů uplatňujících se při procesu formování indikací, je stanoven impuls síly jako směrodatná veličina pro vyhodnocení generovaného magnetického pole. Nová metoda vyhodnocení magnetického pole je založena na vektorovém měření a následném výpočtu impulsu síly na detekční částici. Navržená metoda umožňuje predikovat vliv různých faktorů na kvalitu indikace. ISO norma požaduje nepoužívat magnetizační proudy s činitelem amplitudy větším než tři, bez dokumentovaných důkazů o funkčnosti techniky. Metoda vyhodnocení kvality indikací za pomoci impulsu nicméně predikuje zanedbatelný vliv amplitudového činitele magnetizačních proudů na kvalitu indikace. Vliv amplitudového činitele na kvalitu indikací byl experimentálně prozkoumán s výsledky v souladu s teorií vyhodnocování magnetického pole za pomoci impulsu.

V závěrečné části je řešeno to jak generovat magnetické pole pro detekci libovolně orientovaných defektů. Je zde navržena metoda poskytující uniformní detekční schopnost ve všech směrech využívající pouze jednokanálový zdroj stejnosměrného nebo střídavého proudu. Tato magnetizační metoda využívá časový multiplex mezi magnetizačními proudovými smyčkami a vede ke zjednodušení syntézy magnetického pole a tedy i ke zjednušení návrhu testovacích zařízení.

Klíčová slova: Magnetická metoda prášková, měření magnetického pole, polarizace magnetického pole, vícesměrová magnetizace, vyhodnocení magnetického pole, činitel amplitudy (crest factor), normy, impuls magnetické síly, kvalita indikace, časový multiplex, generování magnetického pole.

Contents

1 | Introduction

Nondestructive testing (NDT) can be defined as an examination, test, or evaluation performed on any type of test object without changing or altering that object in any way to determine the absence or presence of conditions or discontinuities that may have an effect on the usefulness or serviceability of that object [1]. In terms of methods and techniques NDT relies on different physical phenomena such as electromagnetism, an acoustic emission, thermal emission or the penetration of high-energy radiation through materials and structures [2]. NDT plays an important role in industry, especially in areas such as quality control of the production process, reduction of production costs, or increasing the manufacturer's reputation as a producer of high quality goods. Furthermore, NDT is also applied in structural health monitoring, which helps to prevent accidents and ecological disasters, or strategic device failures.

NDT methods are widely used and the market is estimated to reach 24.3 billion USD by 2027 and to exhibit a compound annual growth rate (CAGR) of 6.5 % over the next eight years according to a study published by Grand View Research [3] in 2020. With growing budgets, it seems promising to scientifically explore this field.

Magnetic Particle Inspection (MPI) is one of the most widely used NDT methods. Of the many different NDT techniques used in industry, liquid penetrant and magnetic particle testing account for about one-half of all NDT [4]. MPI can reveal surface discontinuities in ferromagnetic material, including those too small or too tight to be seen with the unaided eye. Magnetic particle indications formed on the surface of tested object above a discontinuity shows the location and approximate size of the discontinuity. MPI can also reveal discontinuities that are slightly below the surface [5].

The research areas addressed in this thesis are chosen to fill gaps in theory which were discovered during the author's work on the project aimed at the MPI

test bench unit design. The goal of the project was to design a test bench unit capable of arbitrarily oriented defects detection in one MPI cycle. At the early phase of the project the generated magnetic field was evaluated by standard QQI gauges, and the initial idea was to generate a rotating magnetic field with circular or elliptical polarization to get multidirectional detection ability. The evaluation process of the generated magnetic field by QQI gauges was very slow and unsuitable for fast optimization. The solution was to perform vector measurements of the magnetic field to get accurate information about magnetic field distribution. After the first measurements, it was clear that the magnetic field of polarizations other than elliptical can produce a multidirectional indication on the QQI gauge. The next task was to find a metric that would evaluate the magnetic field without using gauges and would tell if the defects of all orientations would be detected. By theoretical analysis, the impulse of the magnetic force was introduced as a key quantity to evaluate magnetic field for MPI because it takes into account magnetic force on a detection particle and its duration. The results predicted by the impulse theory do not always agree with recommendations given by standards. It was needed to closely examine these areas, specifically the impact of the crest factor of thyristor regulated currents on the quality of indication. Finally it was necessary to deal with the generation of magnetic field with omnidirectional detection ability on the complex surfaces meant to be tested. A method of generating a magnetic field capable of detecting defects of all orientations was developed. This method requires only a single channel AC or DC source.

Although MPI has been widely used for many years, the physical processes are still not fully understood, and many empirical relations are used to design testing equipment. Therefore, the thesis aims to provide a theoretical background in chosen parts of the MPI and improve understanding of the process mainly in three areas: magnetic field measurement, magnetic field evaluation and magnetic field generation.

The main goals of the thesis are summarised in the following list:

1. Define the requirements for the magnetic field measurement to get relevant information for the evaluation of MPI performance. Design an instrumentation that meets the requirements.

2. Find a method suitable for fast automated magnetic field evaluation.

3. Define a methodology of automated settings of magnetization currents to achieve omnidirectional detection ability.

The thesis is written as a compilation of papers with linking comments. The chapter State of the Art contains a review of current knowledge. The core of the thesis is in the chapter called Results, which consists of a summary of the papers, a reference to the appropriate paper and additional comments, discussions and detailed information which were not published in the papers. There are three parts in the Results chapter corresponding to the main topics of the thesis. The chapter entitled Conclusion summarizes the obtained results.

Disclaimer: In this thesis, the term *magnetization* is not used as it is defined in classical electromagnetic theory, but in a more general way commonly used in magnetic testing (MT), referring to the magnetic state of an object under test.

2 | State of the Art

Magnetic particle inspection is a non-destructive testing method for the detection of discontinuities in ferromagnetic materials. The MPI process consists of a magnetic flux leakage (MFL) method followed by a visual inspection. The object being tested is magnetised, and detection particles are applied to the surface at the same time. The magnetic field in the tested material is interrupted by a potential discontinuity, and the magnetic leakage flux is generated around the discontinuity. The leakage field is inhomogeneous thereby causing applied ferromagnetic detection particles to be attracted to the discontinuity and gather around the discontinuity to form an indication. Indications are then evaluated under ultraviolet (UV) light. In figure 2.1 examples of an MPI test bench unit and MPI indication can be seen.
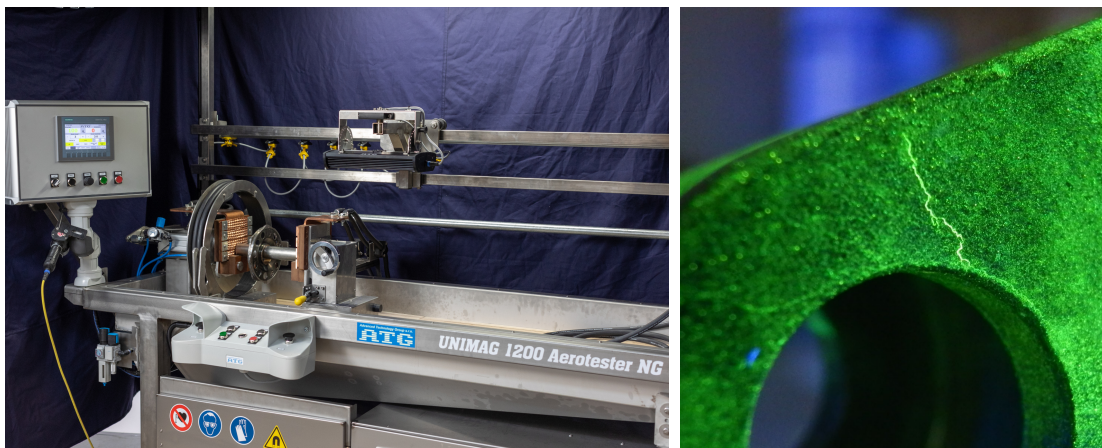
(a) Example of MPI test bench unit (https://atg.cz/)   (b) Example of MPI indication

Figure 2.1: MPI test bench unit and MPI indication

2.1 Magnetic Field Measurement

The recommendations on how to measure magnetic field for MPI can be found in both ISO and ASTM standards. The standards specify only a basic measurement procedure by a single-channel (scalar) gaussmeter. The standards recommend orientation, dimensions and liftoff of the Hall effect element. The process described by the standards does not cover the general case of vector measurement (measurement of both tangential components of magnetic field).

ISO 9934-3 [6] recommends using Hall probes and to consider the orientation of the probe. The plane of the field sensitive element should be kept normal to the surface. If the field varies strongly with height above the surface, it might be necessary to make two measurements at different heights to deduce the value at the surface. To determine the direction and magnitude of the field, the probe shall be rotated to give the maximum reading. Measurement accuracy should be better than 10 %.

ASTM standard E709-15 [7] recommends calibrating Hall effect gaussmeters every six months. A Hall effect sensor should be positioned within 5° of perpendicularity to the tested part. More than one measurement should be taken to ensure consistent readings.

ASTM standard E1444-16 [8] defines the area of the Hall effect probe not to be larger than 5.1 mm by 5.1 mm and should have a maximum centre location 5 mm from the surface. The plane of the probe must be perpendicular to the tested surface within 5°. A holder should be used when performing a magnetic field measurement. The gaussmeter should have a response of 300 Hz or higher. Lack of effective bandwidth could have a significant effect on the resultant value when measuring fields generated by pulse-width modulated MPI equipment. The direction and magnitude of the tangential field on the part surface can be determined by two measurements made at right angles to each other at the same spot.

2.2 Magnetic Leakage Field

MPI relies on leakage field generation around a defect when the tested object is magnetized. There are several analytical models of leakage fields generated by defects. The model based on surface magnetic dipoles was developed by Zatsepin and Shcherbinin [9]. This model was later used by Dutta et al. [10, 11] to calculate the three-dimensional distribution of the leakage field of cylindrical and cuboidal defects. An analytical closed-form solution for the leakage field from a semi-elliptical defect in a linear material has been published by Edwards and Palmer [12]. The article also contains an expression for force components affecting a spherical detection particle.

Many simulations of leakage fields from different defects and magnetization methods have been carried out. A review of FEM simulations related to NDT magnetic methods can be found in [13].

2.3 Magnetic Field Evaluation

Both the intensity and direction of a generated magnetic field for MPI should be tested in order to achieve successful detection. Several approaches are used [5, 1, 14, 15, 16]:

- Pie Gauges

- QQI Shims

- Test Blocks

- Gaussmeters.

These standard indicators are pieces of soft magnetic material with defects of various shapes and dimensions for system performance evaluation. Pie Gauge is one of the most commonly used reference indicators. It consists of a high permeability disc usually divided into six or eight triangular segments separated by gaps, as shown
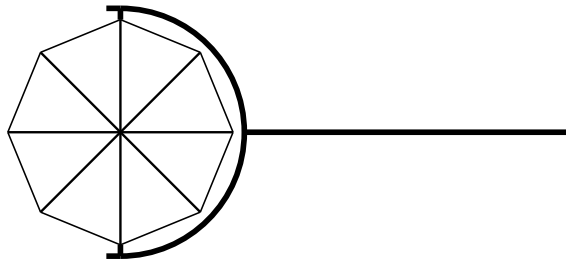
Figure 2.2: Pie Gauge

in Figure 2.2. To protect the gaps, the surface is usually coated by a nonmagnetic layer. The Pie Gauge is placed on the tested object during magnetization, and the applied particles form an indication around the gaps. The Pie Gauge is constructed of a high permeable material, therefore positive indications do not necessarily imply an appropriate magnetic field on the tested surface [7]. The Pie Gauge should be primarily used as an indicator of magnetic field direction.
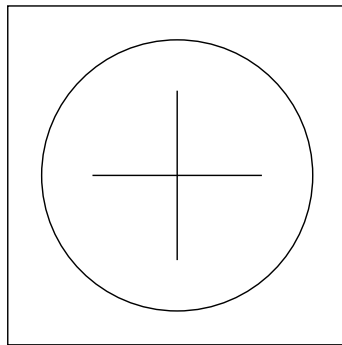

Figure 2.3: Common slot shape of a QQI shims gauge

The Shims Discontinuity Standard (also called Quantitative Quality Indicator (QQI)) consists of thin plates of ferromagnetic materials with artificial slots mimicking defects which indicate the directions of the sufficient magnitude of the generated magnetic field. Shims must be glued onto a tested surface before performance evaluation. Figure 2.3 shows slots of commonly used QQI gauges. Specifications of dimensions and usage can be found in [7].

The other possibility of magnetic field evaluation is to measure the field by a gaussmeter. Most MPI standards include instructions only for scalar magnetic field measurements, i.e., measurements of the field in one direction. The minimal recom-

mended value of the tangential field, which should be sufficient to achieve successful detection, can be found in standards. The ASTM [7] standard recommends the minimal value of the tangential field to be $2.4\,\mathrm{kA/m}$. A slightly lower value $2\,\mathrm{kA/m}$ is recommended by ISO standards [17]. The value is not generally applicable as shown by Raine et al. [18]. Their work proves that successful detection can be achieved by fields of intensity lower than those recommended by the standards.

The standard indicators mentioned are the most commonly used, but generally, any specimen with known defects can be used to evaluate MPI performance. Application of these indicators is time-consuming and technically difficult because they must be placed or fixed on the surface being tested before all the steps of the MPI process are performed. These gauges do not show the exact value of magnetic field. Moreover, it is difficult to verify the whole surface of the material, which should be tested, and the verification of detection ability is limited to the defects of one particular width and depth. The advantage of these indicators over the magnetic field measurement is the evaluation of performance of the whole MPI process, including magnetic suspension quality and UV light characteristics.

When using electromagnetic yoke or permanent magnets, the magnetization force can be checked by the lifting power on a steel plate. The lifting force is specified in [7].

2.4 Magnetic Field Generation and Synthesis

The most important part of every MPI test is magnetization of the tested material. Commonly used methods for magnetic field generation for MPI are [5, 19]:

- direct flow of current through the tested material

- indirect magnetization by coils

- magnetization by permanent magnets

- magnetization by yokes.

Tested materials are magnetized by these methods so that the magnetic flux lines are established within a material. A potential defect interrupts the magnetic flux lines forcing some of the flux lines to leak outside the material, resulting in a so-called magnetic flux leakage created above the defect. The leakage field is inhomogeneous so the applied ferromagnetic detection particles are attracted to the maximum of leakage field and gather around the defect and form an indication. A magnetic field parallel (or close to parallel) to the defect does not create a leakage field. Therefore, according to state of the art methods, a magnetic field should be applied in all directions to detect defects of all orientations. This can be achieved by a vector of the magnetic field rotating at a constant angular velocity and constant magnitude, i.e., by a circular polarization of the applied field in a plane tangential to the tested surface.

The generation of the circularly polarized tangential field to detect arbitrarily oriented defects is described by Japanese researchers in [20]. The rotating field is generated by a magnetizer which consists of six coils situated in the vertices of a regular hexagon. The desired polarization of the field is achieved by passing alternating currents with proper phase shifts through the coils. A similar case is described in [21] where only three coils are used. Measured magnetic field polarizations are presented in both papers.

Much of the research effort in MPI has been directed towards establishing an optimal magnetic field. The optimal applied field generated by the alternating and half-wave rectified current for inspection of welds by magnetic field was investigated by Massa [22]. Massa provided tables of minimum tangential field values to detect subsurface defects for different ways of magnetization and current waveform types.

Oehl and Swartzendruber [23] measured the leakage field from cylindrical defects in non-linear material. They found that the leakage field of the defect does not reach the maximum for the applied field corresponding to the magnetization point of maximal permeability. The applied field where the leakage field reaches a maximum is greater.

There are many recommendations for specific scenarios based on calculations, estimations, simulation and empirical results. There is a lack of generally applicable recommendations on how to generate the magnetic field.

In [24], authors compare the fields generated by the conductor threaded through

10

a pipe. Magnetic field intensity on the surface was measured as a function of the position of the conductor in the pipe. There is only a low variation of magnetic field on the surface of the pipe if the conductor is of the central axis. Contrary to the recommendations in the appropriate British Standards - if insufficient current is available to magnetize a component using a central threading bar, there is no advantage to be gained by the use of a non-central bar. It was shown that the standard recommendations are not generally applicable and any generated magnetic field must be carefully verified.

In [22], the tangential field on the surface of the steel plate was measured for different magnetization methods (prod electrodes, electromagnetic yoke and coil magnetization). Also, the possibility of detection of artificial subsurface defects of different depths was tested. Alternating and single-phase half-wave rectified currents were used.

A defect is optimally detected when a magnetic field is perpendicular to the defect, the point where the strongest leakage field is produced [5, 7], but the orientation of the defect is generally unknown. Several commonly used approaches to magnetic field generation can be used to detect defects of all orientations.

The first method is to perform two full MPI cycles. In the first step, the tested material is magnetized, usually by a yoke or prod electrodes in a certain direction, and all remaining steps of MPI are performed. To detect all defects, the second placement of a yoke or prods rotated by 90° from the first placement is necessary [7, 5]. AC or DC currents can be used. An alternative to this is to rotate the sample under test by 90°. Permanent magnets can also be used with some limitations [1, 15, 7].

A second possible approach, known as multidirectional magnetization, is described in [5]. Multidirectional magnetization can be achieved by several methods, such as the simultaneous combination of different magnetization methods and currents: a combination of DC and AC magnetization, or, a combination of two AC magnetizations. A complex example of how to perform multidirectional magnetization by generating a rotating magnetic field using multiple coils is studied in [20]. The presented solution consists of many coils positioned around the circle powered by three-phase voltage.

Multidirectional magnetization uses a field that changes its direction during the

11

magnetization phase. This approach is based on the intuitive assumption that once the magnetic field flux density vector scans all directions, it becomes perpendicular to any defect at a certain time, making it likely that the defect will be detected. However, the defect can be detected even when the angle between the defect and magnetic field vector is not 90°. A detection method using two MPI cycles to detect arbitrarily oriented defects illustrates this. The angle is usually considered to be at least 45° [1, 25].

3 | Results

The core of the thesis is based on three publications in journals with impact factor. This chapter contains a short summary of papers and additional information and comments not published in the papers. The papers are reprinted in the Appendix - Author's publications.

3.1 Magnetic Field Measurement

Measurement of magnetic field intensity on the surface of the tested material is one possible way how to evaluate the detection ability of the MPI process. Unlike the other evaluation methods, the magnetic field measurement by gaussmeter only evaluates the magnetic field, not the other factors influencing the MPI process. Other factors, such as the quality of detection suspension or UV light characteristics, are not verified. Nevertheless, magnetic field intensity itself should be measured and adjusted at least to satisfy the lower limits specified by the standards [7, 17]. Detection suspension and UV light can be checked independently. The advantage of evaluating magnetic field by gaussmeter is that the verification process is very fast and clean because the application of magnetic particles and evaluation under UV light does not have to be performed. Also, the process of magnetic field synthesis is much faster if only the magnetic field is measured after every current density adjustment.

Commonly available gaussmeters are single-channel devices and, thus, measure only one component of the magnetic field in the direction given by the orientation of the Hall element in the probe. These gaussmeters usually do not provide complete information about magnetic field intensity in time, only the RMS value calculated
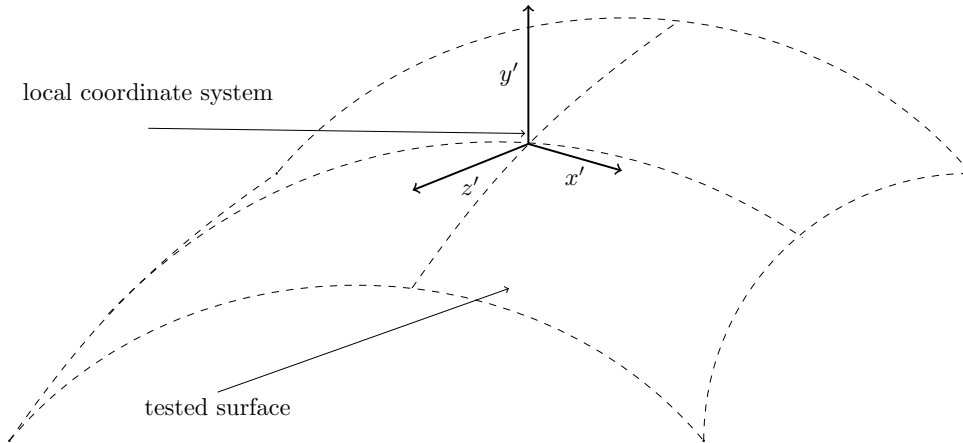
Figure 3.1: Local coordinate system which is used for magnetic field measurement. Plane defined by vectors x' and z' is a tangential plane to the tested surface.

over a certain integration period is available to the user. Single-channel gaussmeters can be used to measure a magnetic field that does not change its direction in time. The measurement must be repeated, and the probe rotated so that the direction of the maximum value of the magnetic field intensity is found. If the magnetic field changes its direction (multidirectional magnetization) it is very difficult to get reasonable results using a single-channel gaussmeter. The probe can be step-by-step rotated to obtain values of the intensity of the magnetic field in several directions. Such a procedure has several significant disadvantages. First, to cover all directions, a large number of measurements is needed, and a problem arises with the precise orientation of the probe and its maintenance in the tangential plane to the surface of the tested material. When performing such a measurement, it is very easy to miss the direction with the minimum or maximum intensity. Single-channel gaussmeters are insufficient for the measurement of magnetic field for multidirectional magnetization. Another problem is that gaussmeters usually only show the RMS value over a certain integration period. The intensity of the magnetic field does not have to be constant during the entire magnetization period for thermal or mechanical reasons. This type of measurement may not find such dependencies.

In order to obtain complete information about the magnetic field relevant for the MPI process, it is necessary to measure both tangential components and record

time-dependant waveforms for the entire magnetization period.

The local coordinate system for magnetic field measurement and evaluation used in this thesis is shown in Figure 3.1. Magnetic field vector generally consists of three components, but only x' and z' are relevant for MPI because these two components are responsible for driving magnetic particles towards the defect on the tested surface. The coordinate system is oriented so that vectors x' and z' are in the tangential plane to the tested surface. For evaluation of detection ability in all directions, it is necessary to measure both $H_{x'}$ and $H_{z'}$ components of the magnetic field. If both components of the magnetic field in the tangential plane are measured, the complete information relevant for evaluation is captured.
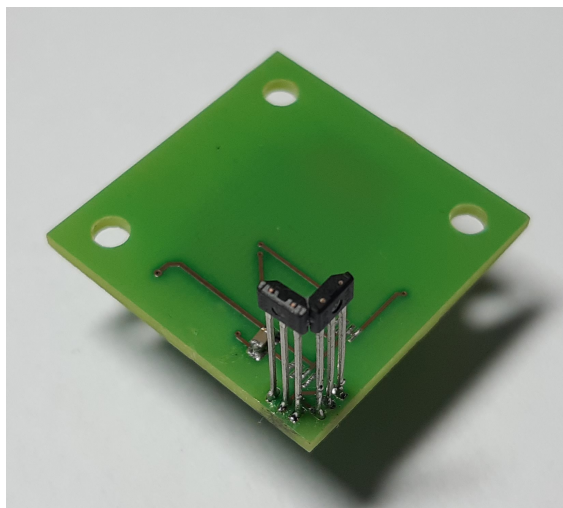

Figure 3.2: First experimental version of a Hall probes holder

All the experiments presented in this thesis required magnetic field to be measured. A two-channel gaussmeter with the sufficient bandwidth and an interface for a transfer of sampled signals to a PC was needed. Instrumentation which meets all requirements is not available in the market so in-house design was needed. The first version of the designed gaussmeter is described in [C1]. All the magnetic field waveforms published in this thesis were measured by this gaussmeter or by the next versions with some modifications and improvements.

The probes of the designed gaussmeter contains two Hall sensors soldered at the PCB perpendicular to each other as shown in Figure 3.2. The local coordinate system is always oriented so that the directions of vectors x' and z' correspond

15

to the sensitivity directions of Hall probes. An analog signal from the probe is amplified and the range of the signal is adjusted for the range of the internal analog to digital converters (ADC) of the STM32F407 microcontroller. Two ADCs are running simultaneously at 10 kHz. Direct memory access (DMA) is used to transfer the samples from the ADCs to a buffer which is sent via USB VCP to PC for processing.

Calibration of the gaussmeter in Helmoholtz coils was done as shown in block scheme in Figure 3.3. The signal generated by the signal generator was amplified by an audio amplifier. The value of magnetic field in Helmholtz coils was calculated from the current running through the coils, which was measured by amperemeter.

Figure 3.3: Gaussmeter calibration scheme

The measurement of magnetic field is very important for the maximization of performance of the MPI and should be done carefully. A field of low intensity or incorrect direction can be responsible for a low percentage of detected defects.

3.2 Evaluation of Magnetic Field

The defect detected by the MPI is indicated by detection particles gathered around. The detection particles are dragged towards the defect due to a force emerging in an inhomogeneous leakage field. Impulse of magnetic force is therefore a key quantity for evaluation of detection ability of MPI to be performed. The idea of evaluation of magnetic field for MPI by calculating impulse was first published in [C2]. The equation for impulse of magnetic force and experimental verification of the new evaluation method can be found in [A1]. The method enables a fast and accurate magnetic field test while neither requiring a QQI shims attachment to the surface,

nor any spraying with particles, nor any subsequent cleaning.

[A1] Pavel Staněk and Zbyněk Škvor. "Automated Magnetic Field Evaluation for Magnetic Particle Inspection by Impulse". In: *Journal of Nondestructive Evaluation* 38.3 (2019). DOI: 10.1007/s10921-019-0615-4

The following equations and comments are related to [A1] but were not published in the article. Equation 6 in [A1] for impulse of magnetic force has a different form which can be used for further analysis of a minimum and maximum of the impulse function. The position of the minimum and maximum can be obtained as a closed-form expression. For general magnetic field vector $\mathbf{H} = (H_x(t), H_z(t))$ the equation for impulse can be rewritten as follows:

$$\frac{|\mathbf{J}(\beta)|}{k} = \int_{t_0}^{t_0+T} \cos(\beta)^2 H_x^2 + 2\cos(\beta)\sin(\beta)H_x H_z + \sin(\beta)^2 H_z^2 \, \mathrm{dt} =$$
$$= \int_{t_0}^{t_0+T} \cos(\beta)^2 H_x^2 + \sin(2\beta)H_x H_z + \sin(\beta)^2 H_z^2 \, \mathrm{dt} =$$
$$= \left(\cos(\beta)^2 \int_{t_0}^{t_0+T} H_x^2 \mathrm{dt} + \sin(2\beta) \int_{t_0}^{t_0+T} H_x H_z \mathrm{dt} + \sin(\beta)^2 \int_{t_0}^{t_0+T} H_z^2 \mathrm{dt} \right).$$
$$(3.1)$$

An equivalent equation for the sampled signal is:

$$\frac{|\mathbf{J}(\beta)|}{k} = \cos^2(\beta)T_s \sum_n H_{xn}^2 + \sin(2\beta)T_s \sum_n H_{xn}H_{zn} + \sin^2(\beta)T_s \sum_n H_{zn}^2 =$$
$$= \cos^2(\beta)T_s \left(\sum_n H_{xn}^2 - \sum_n H_{zn}^2 \right) + \sin(2\beta)T_s \sum_n H_{xn}H_{zn} + T_s \sum_n H_{zn}^2,$$
$$(3.2)$$

where T_s is the sampling period. The first derivative test is used to find extremes of the impulse function:

$$\frac{d|\mathbf{J}(\beta)|/k}{d\beta} = \left(\sum_n H_z^2 - \sum_n H_x^2 \right) T_s \sin(2\beta) + 2 \left(\sum_n H_x H_z \right) T_s \cos(2\beta) \qquad (3.3)$$

$$\frac{d|\mathbf{J}(\beta)|/k}{d\beta} = 0$$

$$\left(\sum_n H_z^2 - \sum_n H_x^2 \right) \sin(2\beta) = -2 \left(\sum_n H_x H_z \right) \cos(2\beta)$$

$$\beta = \frac{\pi m}{2} - \frac{1}{2} \arctan \left(\frac{2 \sum_n H_x H_z}{\sum_n H_z^2 - \sum_n H_x^2} \right), \sum_n H_z^2 \neq \sum_n H_x^2, m \in \mathbb{Z}. \tag{3.4}$$

If $\sum_n H_z^2 = \sum_n H_x^2$ then

$$\beta = \frac{\pi m}{2} - \frac{\pi}{4}, m \in \mathbb{Z}. \tag{3.5}$$

According to equation 3.4, there are four critical points in the interval from 0 to 2π. The function is periodic with period π and therefore the further analysis is limited to this interval. A second derivative is used to determine whether there are local extremes at the critical points:

$$\frac{d^2|\mathbf{J}(\beta)|/k}{d\beta^2} = 2T_s \left(\sum_n H_z^2 - \sum_n H_x^2 \right) \cos(2\beta) - 4T_s \left(\sum_n H_x H_z \right) \sin(2\beta) \tag{3.6}$$

The value of the second derivative at the critical points for $m = 1$ is:

$$2T_s \left(\sum_n H_x^2 - \sum_n H_z^2 \right) \sqrt{ \frac{4 \left(\sum_n H_x H_z \right)^2}{\left(\sum_n H_x^2 - \sum_n H_z^2 \right)^2} + 1 } \tag{3.7}$$

and for $m = 2$ it is:

$$- 2T_s \left(\sum_n H_x^2 - \sum_n H_z^2 \right) \sqrt{ \frac{4 \left(\sum_n H_x H_z \right)^2}{\left(\sum_n H_x^2 - \sum_n H_z^2 \right)^2} + 1 }. \tag{3.8}$$

According to equations 3.7 and 3.8, the type of local extreme can be identified. On the interval from 0 to π there is at most one maximum and at most one minimum.

3.3 Magnetic Field Generation

3.3.1 Thyristor Current Control

Thyristor blocks are a popular choice for current regulation in MPI test bench units. The regulation electronics are relatively simple and offer a sufficient resolution. Load voltage and current can be controlled by adjusting the firing angles of individual thyristors. Numerical simulations of current and voltage waveforms are used to discuss specific details of thyristor regulation. Magnetization circuitry (coils and transformers) are modelled as a serial connection of resistor and inductor as shown in Figure 3.4. In MPI test bench units, the typical values of loads are units of ohms (Ω) and units or tens of milihenri (mH). Figure 3.5 shows simulated waveforms of voltage and current on a serial RL circuit, where t_o is the firing time of thyristor. Figure 3.6 shows how the RMS value of current changes with firing time t_o. It can be seen that increasing t_o above a certain value (given by the load) has no effect because the current is continuously flowing all the time. The regulation possibilities are, therefore, limited. Figure 3.7 shows how the crest factor (CF) changes with t_o. The curves are simulated for the same values of R and L as in Figure 3.6.
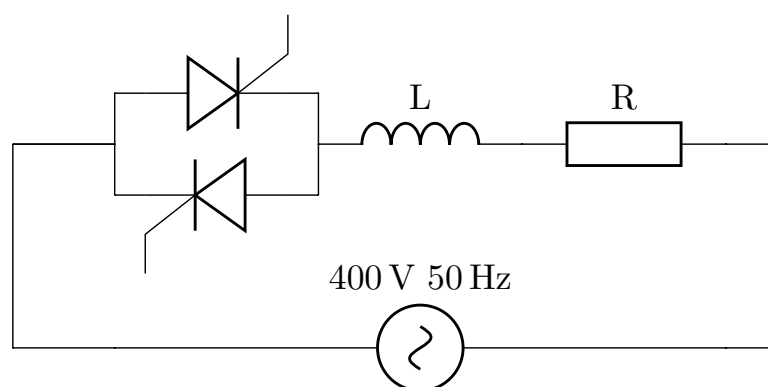

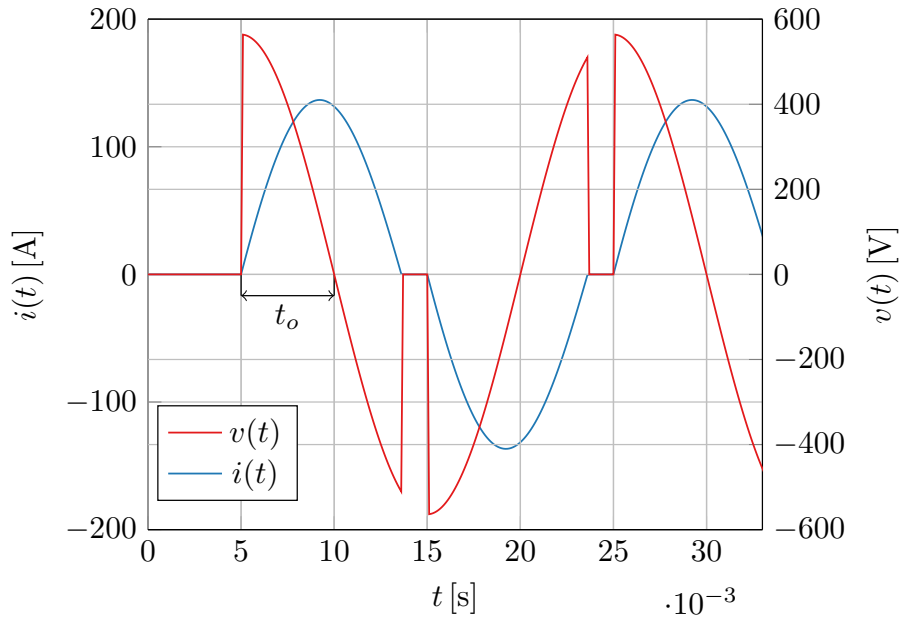Figure 3.4: Thyristor regulation circuit with coil/transformer modelled as RL serial circuit

Figure 3.5: Current through RL circuit controlled by thyristor, $R = 1\,\Omega$, $L = 10\,\mathrm{mH}$

3.3.2 Crest Factor of Current

ISO standard [17] recommends not to use current waveforms with CF > 3 without documented evidence of the effectiveness. When using multidirectional techniques, it is recommended to use a sinusoidal current or phase-controlled current, but the phase cutting should not be more than 90°, which corresponds to $t_o > 5\,\mathrm{ms}$. From Figure 3.6 it can be seen that there is almost no space for current regulation for $t_o > 5\,\mathrm{ms}$ if the values of R and L are around the simulated (realistic) values. To have a wide regulation range of current, the recommendation for limited phase cutting cannot be met. Furthermore, the impulse evaluation method predicts that the CF of the current waveform has a negligible effect on indication quality. The impact of CF on the quality of the indication is investigated in [A2].

[A2] Pavel Staněk and Zbyněk Škvor. "Impact of crest factor on indication quality in the magnetic particle inspection process". In: *Nondestructive Testing and Evaluation* 38.1 (2022). DOI: 10.1080/10589759.2022.2066663
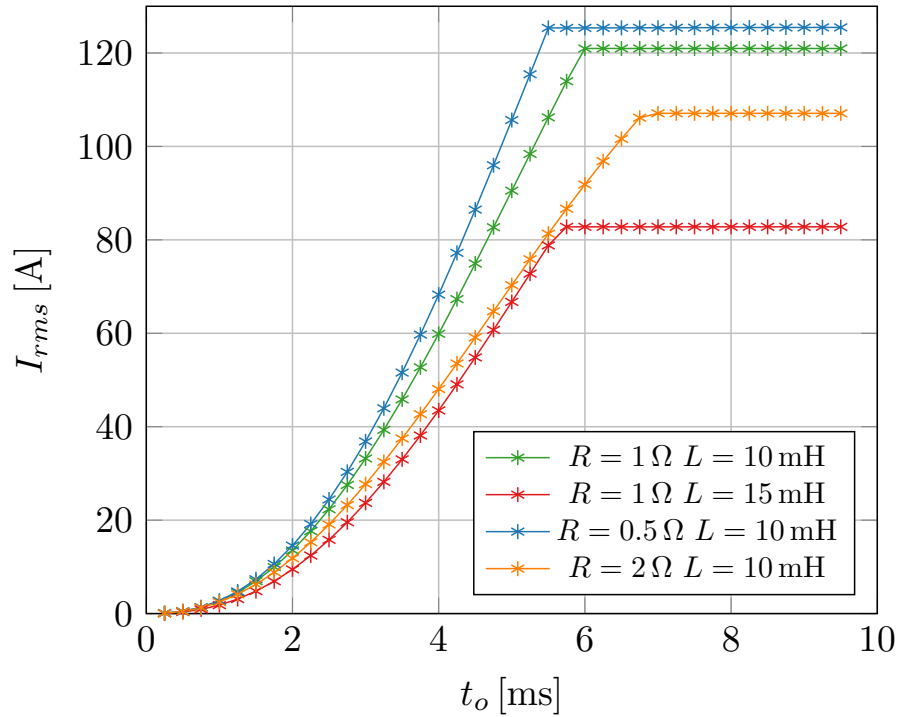
Figure 3.6: RMS value of a current through the RL circuit as a function of firing time

3.3.3 Time-multiplexing of Currents

Designing MPI test bench units is a challenging process with many degrees of freedom. Therefore, a way to simplify the magnetic field optimization was sought. To create multidirectional magnetization, it is necessary to use at least two current loops, but usually more than two are needed. In this case, a time-multiplexing of currents between these loops can be used. The article [A3] describes a way how to simplify the magnetic field optimization using time-multiplexing.

The approach of running a current through only one loop at a certain time brings a number of advantages. The first advantage is that if the total RMS value of the current increases, the impulse does not decrease. If the time-multiplex is not used, then, in some cases, the impulse may decrease even if the RMS value of the currents increases. Another advantage is that the mutual inductive coupling between the individual loops has no effect. Furthermore, this method can generate multidirectional indications using only a single-channel AC or DC source. The
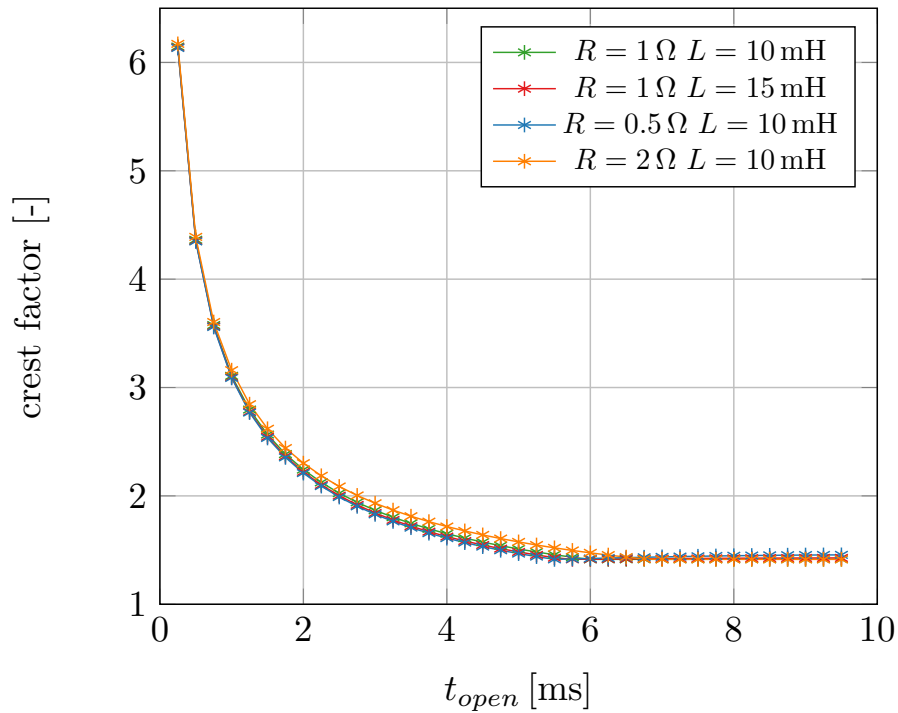
Figure 3.7: Crest factor of current waveform through RL circuit as a function of firing time

last and the most important advantage is the simplification of the magnetic field optimization process. Due to the elimination of the mutual coupling of the current loops, it is possible to first measure the contributions of the magnetic fields from individual channels for different current magnitudes and then calculate the resulting magnetic field as a linear combination of the contributions from individual loops. Thus, magnetic fields can be easily optimized for the entire state space of current magnitudes for all loops. In the case of an AC power supply, the result is independent of the voltage phase.

[A3] Pavel Staněk and Zbyněk Škvor. "Time Multiplexing of Currents for Magnetic Particle Inspection". In: *Research in Nondestructive Evaluation* (2022). DOI: 10.1080/09349847.2022.2132336

The following information and discussion about magnetic field optimization are related to the article, but were not published in the article. In the article, normalized impulse $|\mathbf{J}(\beta)|/k$ is used because k is generally unknown. k is a function of local

spatial coordinates, permeability of the material, defect dimensions and a radius of detection particle. In practice, the exact value of impulse generating clearly visible indication is needed to define an acceptable lower bound for optimization. This value can be experimentally obtained. Test bench units are usually built upon customers' requests to test a specific product. The shape and material of the tested product and the smallest or typical defect are therefore known and can be used for experiments. A setup developed for the experimental measurement of k is presented in [C3]. The calibration setup can be used to find a minimum acceptable value of $|\mathbf{J}(\beta)|/k$ for the optimization process.

During the process of automated magnetic field optimization, the normalized impulse patterns should be compared to each other. The loss function can be used to map values of impulses for different angles onto a real number. The impulse should be above the lower bound and balanced in all directions. The suggested loss function for impulse patterns is:

$$K = \sum_{\beta}^{M} \begin{cases} J'(\beta) - J'_{max} & J'(\beta) > J'_{max} \\ 0 & J'_{max} > J'(\beta) > J'_{min} \\ 10(J'_{min} - J'(\beta)) & J'(\beta) < J'_{min}, \end{cases} \qquad (3.9)$$

where $J'(\beta) = |\mathbf{J}(\beta)|/k$. The values below lower bound J'_{min} are penalized ten times more because the insufficient impulse can potentially lead to an undetected defect. An undetected defect is a worse scenario than generating a false indication caused by an impulse exceeding the upper limit.

4 | Conclusion

This thesis provides solutions to selected problems related to magnetic particle inspection defined in the Introduction. The problems arose during the design of test bench units and were solved by a theoretical insight into physical processes. The theoretical findings were then always experimentally verified, and practical recommendations for test equipment design were derived.

To obtain complete and comprehensive information about the generated magnetic field for the evaluation detection ability of MPI, measurement of both components in a plane tangential to the tested surface (vector measurement) is necessary. Since instrumentation capable of vector measurement was not available on the market, it was designed.

A new method of magnetic field evaluation has been presented. The method is based on vector magnetic field measurement and the calculation of impulse exerted by a magnetic field on a detection particle. The corresponding force impulses compared well to the QQI shim gauge indications. The method enables a fast and accurate field test while neither requiring a QQI shims attachment to the surface, nor any spraying with particles, nor any subsequent cleaning. This makes the evaluation method substantially faster and well-suited for modern MPI device testing, design, and development, as well as for automated magnetic field generation and optimization.

ISO standard 9934 recommends not to use current waveforms with CF > 3 without documented evidence of their effectiveness. The role of the crest factor predicted by the impulse evaluation theory is negligible (if there is any at all). Particle behaviour during an MPI process has been experimentally investigated, and the results support the theoretical expectations. The demand in ISO 9934-1 does not seem to be fully grounded. The impulse is the most important factor to be carefully controlled.

A method of generating a magnetic field enabling the detection of arbitrarily oriented defects using time-multiplexing has been presented and compared to other commonly used magnetization methods. The experiment supported the theoretical findings that the suggested magnetic field generation method can be used to detect defects of all orientations and requires only a single-channel power source. The method may simplify instrumentation without compromising crack detection and reduces the complexity of the optimization or synthesis of a magnetic field used for testing.

The following list summarises what was done. The numbering corresponds to the goals defined in the Introduction.

1. Magnetic field measurement:

    - Vector measurement of magnetic field is necessary to get relevant information for the evaluation of MPI detection ability

    - Instrumentation for vector measurement of magnetic field was designed

2. Magnetic field evaluation for MPI:

    - Automated evaluation procedure was suggested

    - Effect of crest factor of current waveform on indication quality was studied

3. Generation of magnetic field:

    - Method of generation of magnetic field using time-multiplexing was presented

    - Loss function to evaluate impulse pattern was suggested

In addition to the topics addressed in this thesis, there is room for future research in the field of experimental investigation aimed at the detection of threshold measurements. The threshold of successful detection depends on many factors, and it would certainly be interesting to measure these dependencies. Also, statistical studies focused on the probability of detection have practical applications. In these studies, the human factor responsible for evaluating the generated indications plays

a key role. Machine evaluation of indications can be used to eliminate the human factor. Also, an interesting topic would be to simulate the process of the formation of indications taking into account as many physical effects as possible.

5 | About the Author

Personal Information

Name: Ing. Pavel Staněk
Email: stanepa2@fel.cvut.cz, pavelstanek1234@gmail.com

Education

Doctoral studies in Theoretical Electronics
Czech Technical University in Prague, Czech Republic
Faculty of Electrical Engineering, Department of Electromagnetic Field
9/2017 - now

Master studies in Communications, Multimedia, Electronics
Czech Technical University in Prague, Czech Republic
7/2015 - 6/2017
Thesis topic: Fluxmeter for Defectoscopy Application

Erasmus+, Communications and Multimedia Engineering
Friedrich-Alexander-Universität Erlangen-Nürnberg, Erlangen, Germany
10/2016 - 2/2017

Bachelor studies in Communications, Multimedia, Electronics
Czech Technical University in Prague, Prague, Czech Republic
9/2012 - 6/2015

Work Experience

Researcher in Nondestructive Testing (Magnetic Particle Inspection)
Czech Technical University in Prague, Faculty of Electrical Engineering,
Department of Electromagnetic Field, Czech Republic
2015 - 2021

- Development of software for synthesis and optimization of magnetic field for MPI

- Measurement of magnetic fields

- Design of magnetization circuitry (coils, transformers) to generate a specific magnetic field

- Design of current regulation hardware (power phase control)

Hardware Design Engineer, Researcher
Czech Technical University in Prague, Faculty of Nuclear Sciences and Physical Engineering, Department of Physics, Czech Republic
2017 - now

- Design of readout hardware for pixel semiconductor radiation detectors

- Development of software for readout and processing of data produced by radiation detectors

- Radon measurement (design of electrostatic ion collection system, calibration)

- Electrical and radiation testing of radiation detectors (CERN - ALICE, FAIR - PANDA, BNL - EIC)

Hardware Design Engineer
Freelancer
2020 - now

- Design of devices (hardware and firmware) for measurement of magnetic field for calibration of magnetic particle inspection test bench units

6 | List of Publications

Journal Papers with Impact Factor Related to the Thesis

[A1]   Pavel Staněk and Zbyněk Škvor. "Automated Magnetic Field Evaluation for Magnetic Particle Inspection by Impulse". In: *Journal of Nondestructive Evaluation* 38.3 (2019). DOI: `10.1007/s10921-019-0615-4`.

[A2]   Pavel Staněk and Zbyněk Škvor. "Impact of crest factor on indication quality in the magnetic particle inspection process". In: *Nondestructive Testing and Evaluation* 38.1 (2022). DOI: `10.1080/10589759.2022.2066663`.

[A3]   Pavel Staněk and Zbyněk Škvor. "Time Multiplexing of Currents for Magnetic Particle Inspection". In: *Research in Nondestructive Evaluation* (2022). DOI: `10.1080/09349847.2022.2132336`.

Conference Papers Related to the Thesis

[C1]   Pavel Staněk, Zbyněk Škvor, and Miroslav Roxer. "Experimental Gaussmeter for Circular Magnetization". In: *NDT in progress* (2017), pp. 104–107.

[C2]   Pavel Staněk and Zbyněk Škvor. "The effect of higher harmonic components on MPI process". In: *NDT in Canada* (2018).

[C3]   Pavel Staněk and Zbyněk Škvor. "Experimental setup for MPI sensitivity measurements: First results". In: *NDT in progress* (2019).

Journal Papers with Impact Factor not Related to the Thesis

[B1]   Martin Kaschner et al. "Monte Carlo Simulation of Polonium Ion Collection in Electrostatic Field for the Purpose of Radon Detector Development". In: *Radiation Protection Dosimetry* 198.9-11 (2022), pp. 791–795. DOI: `10.1093/rpd/ncac134`.

[B2]   Pavel Vancura et al. "SpacePix2: SOI MAPS detector for space radiation monitoring". In: *Journal of Instrumentation* 18 (2023). DOI: `10.1088/1748-0221/18/01/C01002`.

[B3]   Jakub Jirsa et al. "Characterization of 3.2 Gbps readout in 65 nm CMOS technology". In: *Journal of Instrumentation* (2023). DOI: `10.1088/1748-0221/18/01/C01055`.

[B4]   Jakub Jirsa et al. "Monte-Carlo simulation of charge sharing in 2 mm thick pixelated CdTe sensor". In: *Journal of Instrumentation* (2023). minor revision.

7 | Bibliography

[1] Charles Hellier. *Handbook of nondestructive evaluation*. McGraw-Hill Professional, 2003.

[2] Mohammad Omar. *Nondestructive Testing Methods and New Applications*. IntechOpen, 2012.

[3] Grand View Research. *Non-Destructive Testing Market Size Worth USD 24.3 Billion By 2027: Grand View Research, Inc.* English. 2020. URL: https://www.grandviewresearch.com/industry-analysis/non-destructive-testing-equipment-services-market.

[4] Flake C Campbell. *Inspection of metals: understanding the basics*. ASM International, 2013.

[5] J Thomas Schmidt and Kermit Skeie. *Nondestructive Testing Handbook: Magnetic Particle Testing*. American Society for Nondestructive Testing, 1989.

[6] International Organization for Standardization. *Non-destructive testing - Magnetic particle testing - Part 3: Equipment*. ISO 9934-1:2015(E). Vernier, Geneva, Switzerland: International Organization for Standardization, 2015.

[7] American Society for Testing and Materials. *Standard Guide for Magnetic Particle Testing*. ASTM E709-15. West Conshohocken, Pennsylvania, USA: American Society for Testing Materials, 2015.

[8] American Society for Testing and Materials. *Standard Practise for Magnetic Particle Testing*. ASTM E1444-16. West Conshohocken, Pennsylvania, USA: American Society for Testing Materials, 2016.

[9] NN Zatsepin and VE Shcherbinin. "Calculation of the magneto static field of surface defects 1.Field topography of defect models". In: *Defecktoskopiya* 5 (1966), pp. 50–59.

[10] Sushant M Dutta, Fathi H Ghorbel, and Roderic K Stanley. "Dipole modeling of magnetic flux leakage". In: *IEEE Transactions on Magnetics* 45.4 (2009), pp. 1959–1965.

[11] Sushant M Dutta, Fathi H Ghorbel, and Roderic K Stanley. "Simulation and analysis of 3-D magnetic flux leakage". In: *IEEE Transactions on Magnetics* 45.4 (2009), pp. 1966–1972.

[12] C Edwards and SB Palmer. "The magnetic leakage field of surface-breaking cracks". In: *Journal of Physics D: Applied Physics* 19.4 (1986), pp. 657–673.

[13] Marek Augustyniak and Zbigniew Usarek. "Finite element method applied in electromagnetic NDTE: A review". In: *Journal of Nondestructive Evaluation* 35.3 (2016), p. 39.

[14] Carl E Betz. *Principles of magnetic particle testing*. Magnaflux Corp., 1967.

[15] IAEA Training Course Series. *Liquid Penetrant and Magnetic Particle Testing at Level 2*. 2000.

[16] David Eisenmann et al. "Fundamental engineering studies of magnetic particle inspection and impact on standards and industrial practice". In: (2014).

[17] International Organization for Standardization. *Non-destructive testing - Magnetic particle testing - Part 1: General principles*. ISO 9934-1:2015(E). Vernier, Geneva, Switzerland: International Organization for Standardization, 2015.

[18] G Raine. "Magnetic particle inspection of pressure vessels and pipelines and associated field strength measurements". In: *British Journal of Non-Destructive Testing* 26 (1984), pp. 420–5.

[19] SK Burke and RJ Ditchburn. *Review of literature on probability of detection for magnetic particle nondestructive testing*. Tech. rep. Defence Science and Technology Organisation, 2013.

[20] K Fukuoka et al. "Consideration of multi-coil type magnetization system for magnetic particle testing of omnidirectional crack in all surfaces of 3D shape test object". In: *Electrical Engineering in Japan* 204.4 (2018), pp. 36–42.

[21] K Fukuoka et al. "Evaluation of magnetic flux density distribution in rotating field type magnetic-particle testing using three-phase AC". In: *Journal of the Japanese Society for Non-Destructive Inspection* 58.3 (2009), pp. 102–107.

[22] GM Massa. "Finding the optimum conditions for weld testing by magnetic particles". In: *Non-Destructive Testing* 9.1 (1976), pp. 16–26.

[23] CL Oehl and LJ Swartzendruber. "On the optimum applied field for magnetic particle inspection using direct current". In: *Journal of Nondestructive Evaluation* 3.3 (1982), pp. 125–136.

[24] C Edward and SB Palmer. "An analysis of the threading bar method of magnetic particle flaw detection". In: *NDT international* 14.4 (1981), pp. 177–179.

[25] Louis Cartz. *Nondestructive testing.* ASM International, Materials Park, OH (United States), 1995.

[26] Paul E Mix. *Introduction to nondestructive testing: a training guide.* John Wiley & Sons, 2005.

List of Abbreviation

ADC	Analog to Digital Converter
CAGR	Compound Annual Growth Rate
CF	Crest Factor
DMA	Direct Memory Access
FEM	Finite Element Method
MFL	Magnetic Flux Leakge
MPI	Magnetic Particle Inspection
MT	Magnetic Testing
NDT	Nondestructive Testing
PCB	Printed Circuit Board
RMS	Root Mean Square
UV	Ultraviolet

List of Figures

8 | Appendix - Author's publications

Authors's publications in journals with impact factor related to the thesis.

Automated Magnetic Field Evaluation for Magnetic Particle Inspection by Impulse

Pavel Staněk[1] · **Zbyněk Škvor**[1]

Abstract

A new method of magnetic field evaluation for magnetic particle inspection is presented. Measurements show that a magnetic field value itself is not a sufficient predictor of detection ability. The evaluation method is based on a magnetic field measurement and the calculation of the impulse of magnetic force on a detection particle. Results are compared with commonly used gauges. Directions of sufficient field indicated by this novel method correspond with directions shown by standard gauges.

Keywords Magnetic particle inspection · Magnetic field evaluation · Magnetic field polarization · Probability of detection

1 Introduction

Magnetic particle inspection (MPI) is a non-destructive method widely used for ferromagnetic materials testing where a tested material is magnetized by a magnetic field of sufficient magnitude. A potential defect interrupts the magnetic flux lines established in the material forcing some of the flux lines to leak outside the material, resulting in a so-called leakage field created above the defect. The leakage field is inhomogeneous therefore causing applied ferromagnetic detection particles to be attracted to the defect and gather around the defect to form an indication. A magnetic field parallel (or close to parallel) to the defect does not create such a leakage field and, therefore, a magnetic field should be applied in all directions of the desired detection. This can be optimally achieved by a vector of the magnetic field rotating at a constant angular velocity and constant magnitude, i.e., by a circular polarization of the applied field in a plane tangential to the tested surface. Further information about MPI can be found for example in ref. [1].

Magnetic fields for MPI are usually generated either directly by a current flowing through a tested material,

or, indirectly by coils. These methods are summarized in refs. [2,3]. Traditionally, magnetizers have been developed and tested during design, and then repeatedly used for MPI tests of similar steel parts. The topic was considered mature and disappeared from publications in late 80's.

Since then, technology has moved forward. Progress in informatics and artificial intelligence has made possible new approaches while advanced manufacturing and Industry 4.0 needs handling complex tasks, before unprecedented. New instrumentation for MPI should automatically create magnetic fields to test parts of different shapes, often beyond limits of classic MPI. These devices are required to self-test the magnetic field upon curved surfaces using a robotic arm and proper magnetic sensors. Therefore, a new method of magnetic field evaluation is needed.

Currently used magnetizers are fed by power switching sources from a 50 or 60 Hz power grid. Switching sources are small, easy to control, effective and cheap, though using the switching sources leads to non-sinusoidal currents with higher harmonic components. The presence of such currents generate non-sinusoidal magnetic fields and non-circular polarizations.

Both the intensity and direction of the generated magnetic field for MPI should be tested to achieve successful detection. Several approaches are used [4,5]:

– Pie gauges
– QQI shims
– Test blocks
– Gaussmeters.

Pavel Staněk
stanepa2@fel.cvut.cz

Zbyněk Škvor
skvor@fel.cvut.cz

[1] Department of Electromagnetic Field, Faculty of Electrical Engineering, Czech Technical University in Prague, Technická 2, 166 27 Prague 6, Czech Republic

All the gauges and test blocks are pieces of soft ferromagnetic materials with artificial defects of various shapes. The verification of a magnetic field is limited to the particular defect shape and the gauges do not provide quantitative data on the intensity of an applied magnetic field. All MPI steps must be performed during the evaluation process. Moreover, it is also complicated to verify the whole surface of a tested material and almost impossible to verify magnetization of curved surfaces.

Another possibility of how to verify a magnetic field is to measure intensity by a gaussmeter. Most instrumentation available on the market provide only RMS value(s) in one (or three) direction(s), thus a significant amount of information about magnetic fields remains unknown.

A successful application of MPI requires the optimization of two important quantities:

– Magnetic field distribution
– Duration of the presence of the magnetic field.

The magnetic field distribution is a function of both the magnitudes and phases of the feeding currents. Another important parameter of an MPI test is the time duration of the applied field. The force driving the detection particles towards a defect needs enough time to form a sufficient indication. A simulation of this process can be found in ref. [6].

A single quantity—the impulse of the force on a detection particle—combines these two quantities into one in a way that provides clear insight into the process. In the following chapters a new method for magnetic field verification is presented. This method is based on a vector magnetic field measurement and data postprocessing, i.e., the calculation of an impulse on a spherical detection particle [7].

Probability of detection (POD) as defined in ref. [3] or in ref. [8] is a statistically evaluated function of probability of defect detection depending on defect length. Details of application of MPI such as magnetization method, magnetic field direction and strength, and detection particles used are not mentioned in these studies. Only average performance of MPI is evaluated [3]. However, the proper application of MPI is essential for successful detection. The new method of magnetic field evaluation suggested in this paper can be used to optimize MPI application and increase the POD to get closer to the ideal case described in ref. [9].

Force Exerted on a Detection Particle

The detection particles are dragged towards the defect due to a force emerging in an inhomogeneous leakage field. An analytical closed-form solution for the force components affecting a spherical detection particle, due to a leakage field created by a semi-elliptical defect in a linear material, has
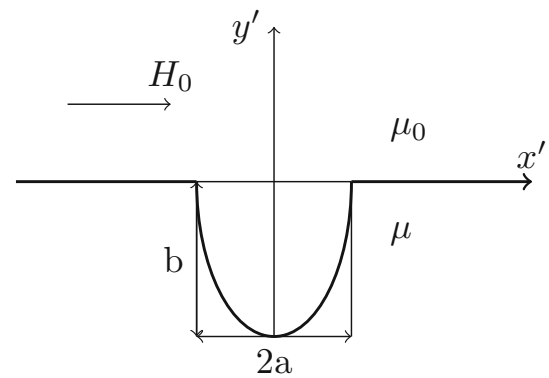

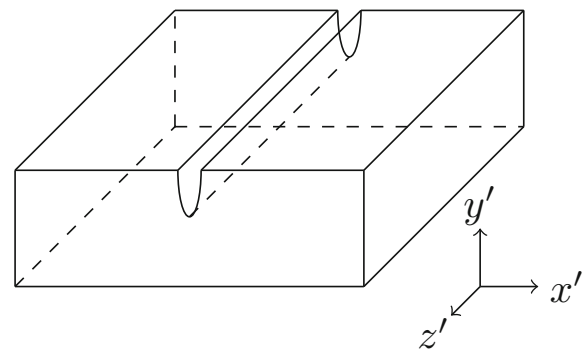**Fig. 1** Semi-elliptical defect in local coordinates

**Fig. 2** Semi-elliptical defect and coordinates system orientation

been published by Edwards and Palmer [10]. The defect is considered to be infinitely long in z' direction. Figure 1 depicts a semi-elliptical defect in local coordinates x', y'. The complete 3D situation can be seen in Fig. 2. $F_{x'}$ is an important force component because it moves the detection particle towards the defect:

$$F_{x'} = -\frac{8}{3}\mu_0\pi r^3 \left[(H_0 + H_{x'})\frac{\partial H_{x'}}{\partial x'} + H_{y'}\frac{\partial H_{y'}}{\partial x'} \right], \qquad (1)$$

where r is a detection particle radius, H_0 is the field applied along axis x', and $H_{x'}$ and $H_{y'}$ are leakage field components. The derivation and full equations for $H_{x'}$, $H_{y'}$ and $F_{x'}$ can be found in ref. [10]. Since the expressions for components $H_{x'}$ and $H_{y'}$ contain H_0^2, it can be factored out:

$$F_{x'} = -\frac{8}{3}\mu_0\pi r^3 H_0^2 \left(\frac{\partial \bar{H}_{x'}}{\partial x'} + \bar{H}_{x'}\frac{\partial \bar{H}_{x'}}{\partial x'} + \bar{H}_{y'}\frac{\partial \bar{H}_{y'}}{\partial x'} \right) =$$
$$= kH_0^2, \qquad (2)$$

where k is function of local spatial coordinates x' and y', a permeability of material μ, defect dimensions a and b, a radius of detection particle r, $\bar{H}_{x'} = H_{x'}/H_0$, and $\bar{H}_{y'} = H_{y'}/H_0$. The spatial dependence of a force on a spherical particle of radius 0.1 mm situated 1 mm above the surface
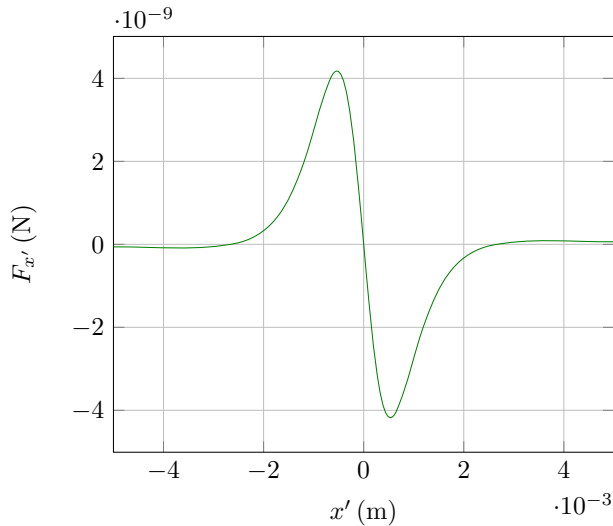
Fig. 3 Magnetic force on a spherical detection particle of radius 0.1 mm, 1 mm above the surface in a leakage field created by a semi-elliptical defect (a=0.1 mm and b=1 mm). The applied field $H_0 = 1000$ A/m

Fig. 4 Defect and **H** vector orientation in xz plane

(a=0.1 mm and b=1 mm) is shown in Fig. 3. Relative material permeability μ is 1000 and the applied field H_0 is 1000 A/m.
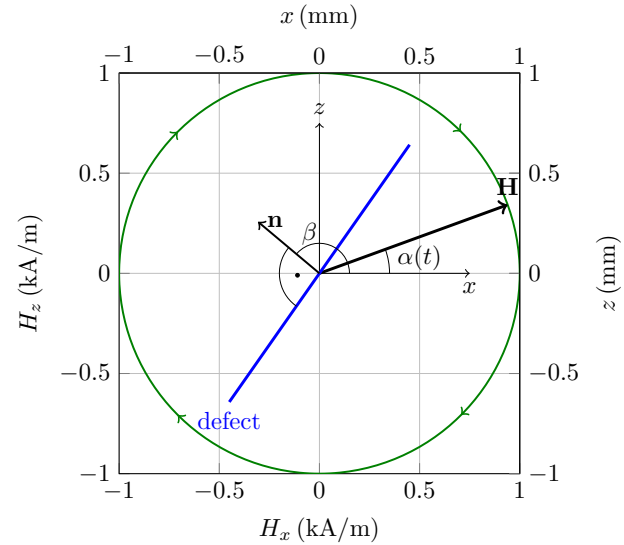
Generally any other equation describing leakage field generated by a defects of different shape can be used. In ref. [11] can be found the expression for the leakage field of a rectangular slot. In the following chapters of this study the coefficient k is not evaluated and is treated as a general function of a leakage field, detection particle radius and permeability in all calculations.

Impulse Calculation

Multi-directional magnetizers are usually fed from a power grid, therefore tested materials are magnetized by 50/60 Hz (European/US standard) currents. Modern magnetizers often make use of switched-mode power supplies. In most cases the tested materials are non-linear. Both facts provide for higher harmonic component generation whereby the magnetic field is no longer sinusoidal. This effect can be described by a Fourier series.

First, let us define the global coordinate system first. The infinite boundary between air and material of permeability μ is located in a xz plane at a position where $y = 0$. In this plane the components of vector **H** are defined by a Fourier series as follows:

$$H_x = \frac{a_0}{2} + \sum_{n=1}^{\infty} a_n \cos(2\pi n f t) + \sum_{n=1}^{\infty} b_n \sin(2\pi n f t))$$

$$H_y = 0 \tag{3}$$

$$H_z = \frac{c_0}{2} + \sum_{n=1}^{\infty} c_n \cos(2\pi n f t) + \sum_{n=1}^{\infty} d_n \sin(2\pi n f t),$$

where f is the base frequency and t stands for time. Equation (3) describes the polarization of magnetic field **H** in a plane tangential to the surface of a tested material, i.e., in the xz plane at $y = 0$. The basic (and as for MPI ideal) polarization is a circular polarization defined by only two non-zero coefficients a_1 and d_1. A situation with coefficients $a_1 = d_1 = 1$ is depicted in Fig. 4. As described in the previous section the leakage field created by a field perpendicular to the semi-elliptical defect is known. If the magnetic field vector **H** is rotating in the tangential plane, vector **n** needs to be defined to calculate H_0 which is the projection of **H** in a direction perpendicular to the defect. Let **n** be a unity vector perpendicular to a arbitrary oriented defect: $\mathbf{n} = (\cos(\beta), 0, \sin(\beta))$, where β is an angle between **n** and positive semi-axis x. If the magnetic field polarization is described by (3), the projection of vector **H** in the direction of vector **n** can be calculated as follows:

$$H_0 = ||\mathbf{H}|| \cos(\beta - \alpha) = ||\mathbf{H}|| \frac{\mathbf{H} \cdot \mathbf{n}}{||\mathbf{H}|| \, ||\mathbf{n}||} = \mathbf{H} \cdot \mathbf{n}, \tag{4}$$

where $\beta - \alpha$ is an angle between vectors **H** and **n**. This situation is depicted in Fig. 4.

Impulse is the desired quantity describing detection ability and is defined as:

$$\mathbf{J} = \int_{t_1}^{t_2} \mathbf{F} dt. \tag{5}$$

If magnetic field is considered to be periodical, the relevant quantity is obtained by integration over one base period. The final impulse is then obtained as a product of this result and the number of periods. However, measurements have proven
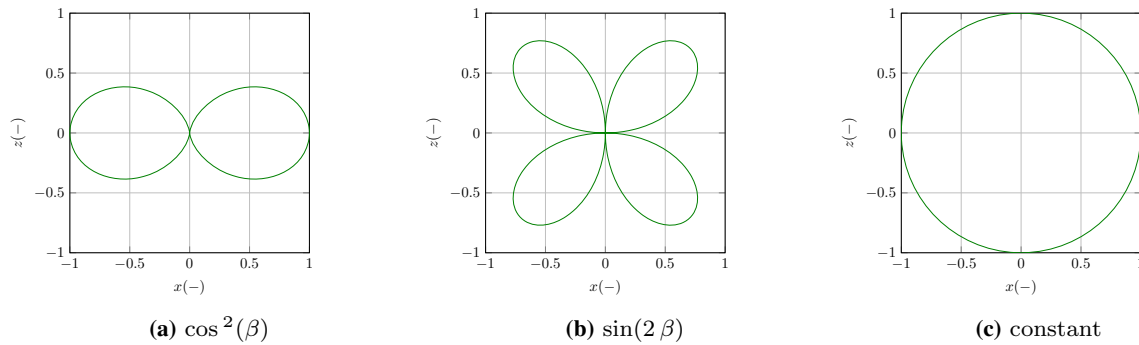
(a) $\cos^2(\beta)$ **(b)** $\sin(2\beta)$ **(c)** constant

Fig. 5 Polarizations in polar coordinates

that real magnetizers may provide such currents that require integration over the whole magnetizing event instead.

To calculate the impulse dragging a detection particle towards a defect, Eq. (2) is inserted into definition (5), to give:

$$
\mathbf{J}(\beta) = \int_{t_0}^{t_0+T} F_{x'}(\mathbf{H}(t)) \mathrm{d}t = \int_{t_0}^{t_0+T} k H_0^2(t) \mathrm{d}t =
$$
$$
= k \int_{t_0}^{t_0+T} (\mathbf{H}(t) \cdot \mathbf{n})^2 \mathrm{d}t,
$$
(6)

where $T = 1/f$ is the base period. Vector components H_x and H_z are measured, therefore all non-linear and dynamic effects are already included and Eq. (2) for force $F_{x'}$ can be used. The impulse is then:

$$
\mathbf{J}(\beta) = \int_{t_0}^{t_0+T} k H_0^2 \mathrm{d}t = k \int_{t_0}^{t_0+T} (\mathbf{H}(t) \cdot \mathbf{n})^2 \mathrm{d}t
$$
$$
= k \int_{t_0}^{t_0+T} \Big(\cos(\beta) H_x + \sin(\beta) H_z \Big)^2 \mathrm{d}t
$$
$$
= \frac{k}{2f} \bigg[\cos^2(\beta) \bigg(\sum_{n=1}^{\infty} \big(a_n^2 + b_n^2 - c_n^2 - d_n^2 \big)
$$
$$
+ 2a_0^2 - 2c_0^2 \bigg)
$$
$$
+ \sin(2\beta) \bigg(\sum_{n=1}^{\infty} \big(a_n c_n + b_n d_n \big) + 2a_0 c_0 \bigg)
$$
$$
+ \sum_{n=1}^{\infty} \big(c_n^2 + d_n^2 \big) + 2c_0^2 \bigg],
$$
(7)

where f is $1/T$. Equation (7) is the impulse on a detection particle in a direction given by angle β and shows the detection ability of MPI in this direction. The result (7) contains three terms. The first term modulated by $\cos^2(\beta)$ is shown in Fig. 5a and plotted in polar coordinates. There are two blind angles in detection ability, i.e., directions of zero detection ability. These two angles are $90°$ and $180°$ in Fig. 5a.

The second term modulated by $\sin(2\beta)$ is in Fig. 5b. The frequency is doubled, therefore there are four blind angles with zero detection ability. The remaining term in Fig. 5c is independent of angle β and improves the detection ability in all directions. The resulting impulse is a summation of these three terms multiplied by coefficients from a Fourier series. This solution seems to respect the symmetrical patterns shown by QQI shims or Pie Gauges in most cases with the only exception being when a gauge is placed exactly at the border of sufficient field.

The square of definition of RMS value

$$
H_{RMS}^2 = \frac{1}{T} \int_{t_0}^{t_0+T} H(t)^2 dt
$$
(8)

differs from Eq. (6) only by the term kT. The RMS value of the magnetic field in a certain direction integrated over the whole duration of the test is proportional to the impulse.

Implementation and Experimental Results

In practice only samples of a magnetic field are usually known, therefore a numerical algorithm is required. Equation (6) must be solved by a numerical method. First the square of the inner product is calculated for all desired directions given by angle β. Then the numerical integration over the samples of magnetic field $\mathbf{H}$ is performed. To determine the exact value of impulse the multiplicative coefficient k must be estimated. Coefficient k varies with spatial coordinates, used magnetic particles, expected defect sizes and tested material permeability. To achieve a high detection probability the coefficient should be estimated for the worst expected case.

The threshold of detection ability (minimal value of impulse to clearly see an indication) is represented by a circle with a centre in the origin of coordinates in a polar plot of impulse. To determine this threshold for a given detection particles, defect size, and defect orientation, exact measurement is needed.
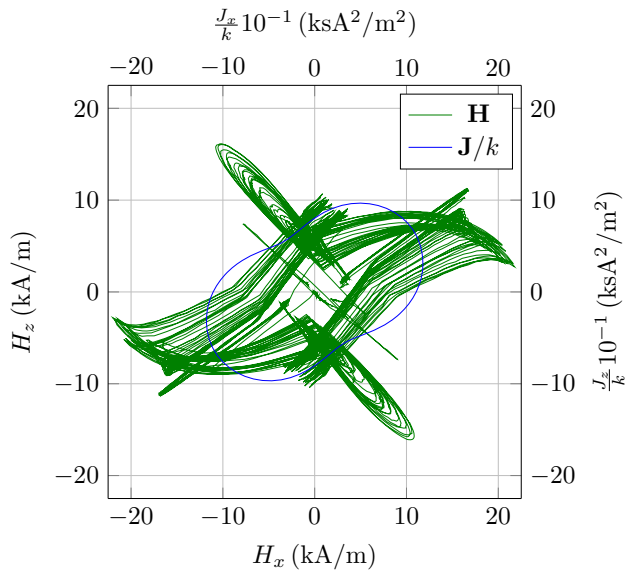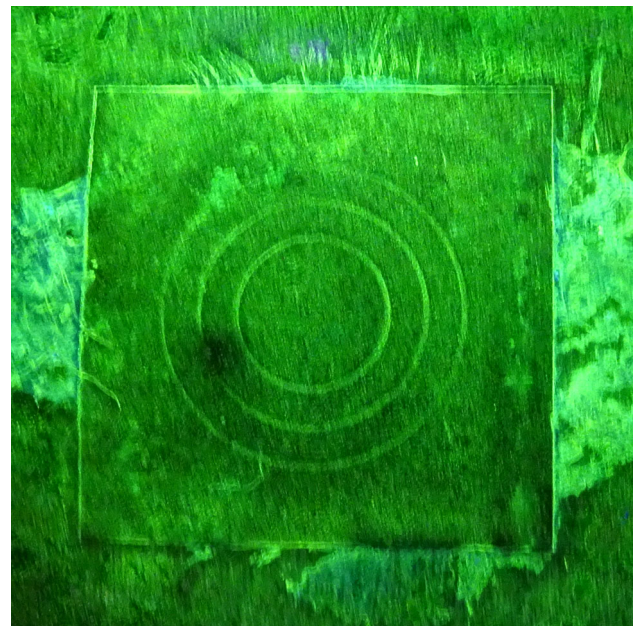
Fig. 6 Magnetic field polarization and impulse curve (Color figure online)

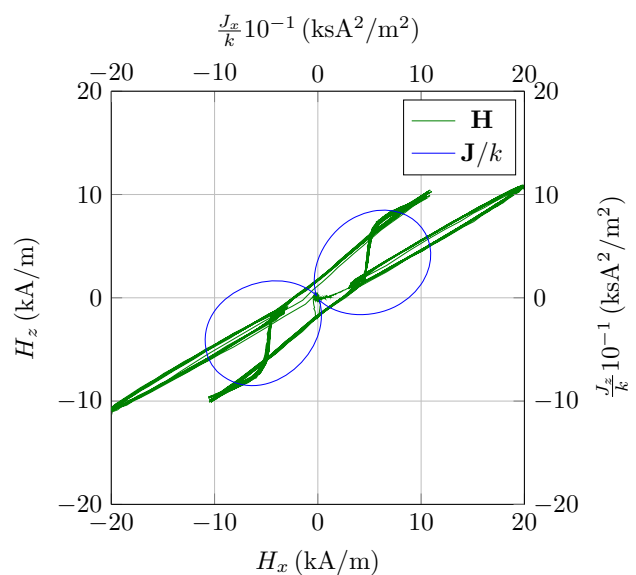**Fig. 7** QQI shim detection pattern corresponding to the polarization in Fig. 6

The initial results of the measurements and their post-processing are presented to verify the idea of evaluating magnetic field detection ability by calculating impulse on a detection particle and comparing it with QQI shims indication patterns. Two different magnetic fields generated by a multi-coil magnetizer were measured at the same point on the steel pipe where a QQI shim was placed. The tested pipe was magnetized by two coils perpendicular to each other. A current source was fed from a 50 Hz power grid and the magnitudes were regulated by thyristors.

For the first measurement the currents were set to achieve fully circular detection pattern by the QQI shim. The tested pipe was magnetized for 1 s and 10k samples of a magnetic field in both x and z directions were taken. During the first measurement the magnitudes of field changed, therefore the polarization in Fig. 6 (green) also changed. If all the periods of field waveforms had the same magnitude during the test, the polarization would be a single-path curve. The QQI shim from the first measurement showed fully circular indication (Fig. 7). The impulse $\mathbf{J}$ divided by coefficient k calculated by a numerical method in Fig. 6 (blue), do not have any blind angles and the threshold circle is completely inside the impulse curve which indicates sufficient detection ability in all directions.

For the second measurement the currents were set so that the QQI shim showed only partial indication. The results are depicted in Figs. 8 and 9 in the same manner as in the previous case. The currents were more stable than in the previous case so the polarization is nearly a single-path curve. The impulse $\mathbf{J}/k$ curve has two blind angles and it can be seen that the blind angles indicated by the QQI shim are very similar to the blind angles indicated by impulse. The threshold circle,

Fig. 8 Magnetic field polarization and impulse curve (Color figure online)

which should have been measured to determine the exact blind angles, intersects the impulse curve.

The polarizations from Figs. 6 and 8 were generated by time-dependant components containing odd-integer harmonics of a base frequency $f = 50 Hz$. The content of even harmonics in the signals is close to zero. Table 1 shows the ratio of odd harmonics normalised to the first at 50 Hz.
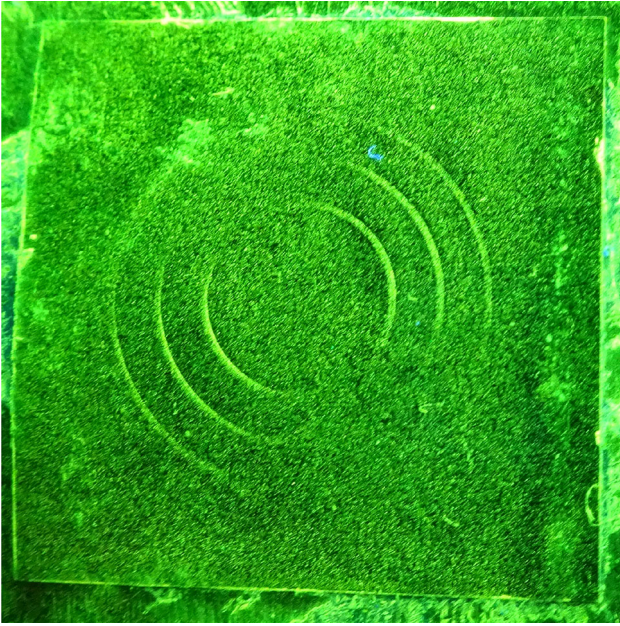
Fig. 9 QQI shim detection pattern corresponding to polarization in Fig. 8

Table 1 Harmonic components of $H_x(t)$ and $H_z(t)$

Harmonic component		1st	3rd	5th	7th	9th	11th
First measurement	H_x	1	1.02	0.34	0.15	0.07	0.02
	H_z	1	0.34	0.21	0.07	0.05	0.03
Second measurement	H_x	1	0.69	0.19	0.11	0.05	0.05
	H_z	1	0.84	0.12	0.12	0.05	0.05

Conclusion

A new method of magnetic field evaluation has been presented and experimentally verified. The method is based on magnetic field measurements and the calculation of impulse exerted by a magnetic field on a detection particle. Measurements of two complex magnetic fields were presented. The corresponding force impulses compared well to the QQI shim gauge indications.

The method enables a fast and accurate field test while neither requiring a QQI shims attachment to the surface, nor any spraying with particles, nor any subsequent cleaning. This makes the method substantially faster and well-suited for modern MPI device testing, design, and development, as well as for automated magnetic field generation and optimization.

References

1. Lovejoy, M.: Magnetic Particle Inspection: A Practical Guide. Springer, New York (2012)
2. Schmidt, J.T., Skeie, K.: Nondestructive Testing Handbook: Magnetic Particle Testing. American Society for Nondestructive Testing, Columbus (1989)
3. Burke, S., Ditchburn, R.: Review of literature on probability of detection for magnetic particle nondestructive testing. Tech. rep., Defence Science and Technology Organisation (2013)
4. Hellier, C.: Handbook of Nondestructive Evaluation. McGraw-Hill Professional, New York (2003)
5. IAEA Training Course: Liquid penetrant and magnetic particle testing at level 2 (2000)
6. McCoy, J., Tanner, B.: Simulation of particle trajectories in magnetic particle inspection. IEEE Trans. Magn. **24**(2), 1665–1667 (1988)
7. Staněk, P., Škvor, Z.: The effect of higher harmonic components on MPI process. NDT in Canada 2018, Proceedings (2018)
8. Zolfaghari, A., Zolfaghari, A., Kolahan, F.: Reliability and sensitivity of magnetic particle nondestructive testing in detecting the surface cracks of welded components. Nondestr. Test. Eval. **33**(3), 290–300 (2018)
9. Omar, M.: Nondestructive Testing Methods and New Applications. IntechOpen, Rijeka (2012)
10. Edwards, C., Palmer, S.: The magnetic leakage field of surface-breaking cracks. J. Phys. D **19**(4), 657–673 (1986)
11. Zatsepin, N., Shcherbinin, V.: Calculation of the magneto static field of surface defects. Defectoskopiya **5**, 50–59 (1966)

Impact of crest factor on indication quality in the magnetic particle inspection process

Pavel Staněk & Zbyněk Škvor

Published online: 27 Apr 2022.

Submit your article to this journal ⏎

View related articles ⏎

View Crossmark data ⏎

Taylor & Francis
Taylor & Francis Group

Check for updates

Impact of crest factor on indication quality in the magnetic particle inspection process

Pavel Staněk [ID] and Zbyněk Škvor [ID]

Department of Electromagnetic Field, Faculty of Electrical Engineering, Czech Technical University in Prague, Prague, Czech Republic

ABSTRACT

Magnetic particle inspection is a well-established industrial process of quality control. The ISO standard for magnetic particle inspection requires control of the crest factor and recommends avoiding current waveforms with a crest factor larger than three without documented evidence of detection effectiveness. Modern test bench units often use thyristor regulation of the magnetization current, which enables broad control ranges to generate an adequate magnetic field. A possible method of evaluation of magnetic field for magnetic particle inspection is to quantify the force effect on a detection particle. The cumulative force effect can be expressed as an impulse of force on a detection particle. The method of evaluation by an impulse of force implies that crest factor does not have a major effect if the impulse is controlled. This work contains a theoretical analysis of force in magnetic field generated by thyristor controlled currents. In the experimental part a comparison of indications generated by magnetic fields of different crest factorsis performed. The results of the experiment are in line with the theoretical analysis and show that it is the impulse that plays the major role in the formation of an indication and not crest factor.

1. Introduction

Magnetic particle inspection (MPI) is a non-destructive testing method for detecting discontinuities in ferromagnetic materials. The MPI process consists of a magnetic flux leakage (MFL) method followed by a visual inspection. The object being tested is magnetised, and detection particles are applied to the surface at the same time. The magnetic field in the tested material is interrupted by a potential discontinuity, and the magnetic leakage flux is generated around the discontinuity. The leakage field is inhomogeneous thereby causing applied ferromagnetic detection particles to be attracted to the discontinuity and gather around the discontinuity to form an indication. Indications are then evaluated under ultraviolet (UV) light.

Standard ISO 9934 [1] contains general principles for MPI and specifies the surface preparation, magnetisation techniques, requirements and application of the detection media, as well as the recording and interpretation of results. All established techniques

---

should be reliable and repeatable. To achieve this the standard recommends: *Where time varying currents (I) are used to produce a magnetic field (which will also be time varying), it is important to control the crest factor (shape) of the waveform and the method of measurement of the current in order to establish a repeatable technique. . . . Waveforms with a crest factor (i.e. I_{pk}/I_{RMS}) greater than 3 shall not be used without documented evidence of the effectiveness of the technique.*

It is essential to generate an adequate magnetic field that results in sufficient force on the detection particles. The method of evaluation of the magnetic field by impulse of force [2] describes the relation between magnetic force and the quality of indication. This method takes into account the two most important quantities (magnetic force and its duration) and implies that crest factor (CF) does not play a role if the impulse is controlled. If the values of the impulses are maintained, the indications should be highly similar. Theoretical results based on this method of evaluation are not in line with the ISO standard.

The experimental section includes a comparison of indications generated by the same values of impulse but with different crest factors of magnetic field waveforms. The experiment was performed using a standard test bench unit for indirect magnetisation by coils. The current waveforms were controlled by thyristors. Images of indications were captured under UV light and, subsequently, compared using methods of image processing.

2. Force impulse in a leakage field

There are several methods on how to evaluate whether the magnetic field is adequate for MPI, including approaches such as pie gauges, QQI shims or gaussmeters [3,4]. The method [2] mentioned in the Introduction and which is applied in this paper is based on the post-processing of the magnetic field measured. In order to evaluate the detection ability of the generated magnetic field in all possible directions (arbitrary defect orientation), a vector measurement of the magnetic field is required, i.e. both orthogonal components of the magnetic field ($H_x(t)$ and $H_z(t)$) in a plane tangential to the tested surface are measured.

Magnetic field strength and magnetisation time must both be taken into account in the evaluation process. The cumulative force effect on a detection particle is quantified by a force impulse:

$$|\mathbf{J}(\beta)| = \int_{t_0}^{t_0+T} k H_0^2(t)\,\mathrm{d}t = k \int_{t_0}^{t_0+T} (\mathbf{H}(t) \cdot \mathbf{n})^2 \mathrm{d}t, \tag{1}$$

where $|\mathbf{J}(\beta)|$ is the impulse in the direction of $\mathbf{n}$, $\mathbf{n}$ is a unity vector perpendicular to a defect, $\mathbf{H}(H_x(t), H_z(t))$ is the magnetic field vector in a plane tangential to the material surface, H_0 is the length of the projection of $\mathbf{H}(t)$ onto a direction of $\mathbf{n}$, T is magnetisation time. k is a function of local spatial coordinates, the permeability of material μ, defect shape and dimensions, and the radius of detection particle r. Figure 1 shows the circular polarisation of the magnetic field vector $\mathbf{H}$ in the xz tangential plane, angle $\alpha(t)$ between the positive semi-axis x and the magnetic field vector $\mathbf{H}$, and angle β between the positive semi-axis x and vector $\mathbf{n}$.
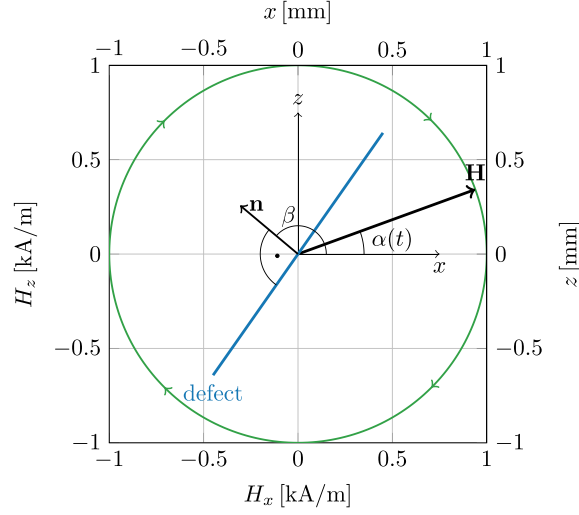
Figure 1. Defect and **H** vector orientation in the *xz* plane.

The square of the RMS value of the time-dependent waveform $H(t)$

$$H_{RMS}^2 = \frac{1}{T} \int_{t_0}^{t_0+T} H(t)^2 \mathrm{d}t \qquad (2)$$

differs from Equation (1) only by the term kT. The square of the RMS value of the magnetic field in a certain direction integrated over the whole duration of the magnetic field presence is proportional to the impulse and is a measure of detection ability.

The force on a detection particle in a leakage field is a complex function of defect shape and subsequent leakage field, the position of a particle in the leakage field, the radius of the particle and the permeability of the particle. In Equation (1) it is represented by function $k\,[kg \cdot m^3/A^2 \cdot s^2]$ which is, generally, unknown. If the MPI is performed under the same conditions (save for magnetic field intensity), k becomes only a multiplicative constant. Therefore $|\mathbf{J}|/k$ is evaluated in the experiment because all other variables affecting k are unchanged during the entire experiment. Knowledge of the value of k is not needed for the experiment.

3. Thyristor regulation and crest factor

Commonly used MPI bench units are powered by a three-phase alternating voltage system (400 V, 50 Hz). Materials being tested can be magnetised directly, using a current flowing through the object, or indirectly, by external coils. The direct magnetisation current is provided by step-down transformers, with a secondary winding connected to the tested specimen. To achieve an optimal magnetic field and maximal
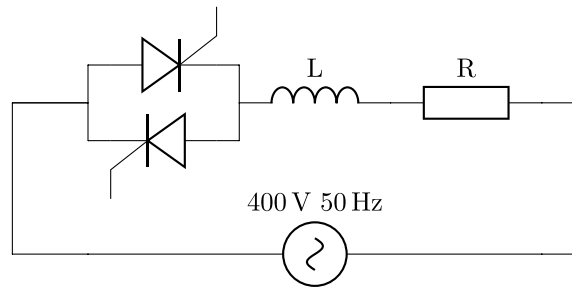
Figure 2. Thyristor regulation circuit.

efficiency the current should be controlled which can easily be done by modern electronics using thyristors. The load voltage and the current can be controlled by adjusting the firing angles of individual thyristors.

Numerical simulations of current and voltage waveforms are used to demonstrate some features of this regulation. The equation describing the circuit in differential form was solved by an integral solver from the *SciPy*, *Python* open-source library. The load (magnetisation coil or step-down transformer) is modelled as an RL serial circuit, as shown in Figure 2. The parameters of the simulated circuit were $R = 1\,\Omega$ and $L = 10\,$mH. The supply voltage is the European standard phase to phase voltage 400 V at 50 Hz. Figure 3 shows an example of the simulated voltage and current waveforms with a firing angle of $90°$. Figure 4 shows the currents as a function of the firing angles. Due to energy accumulation in the inductor, the current flows for a certain time after the voltage crosses
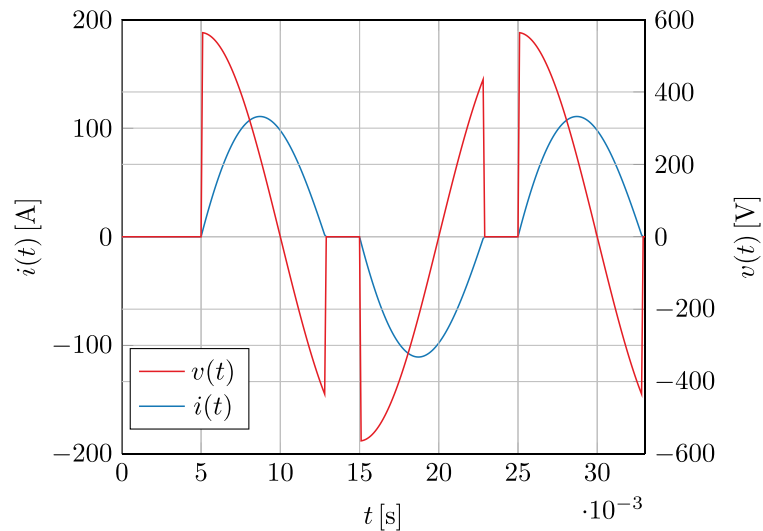

Figure 3. Current and voltage on the RL serial circuit in Figure 2. Supply voltage is 400 V AC, $R = 1\Omega$, $L = 10\,$mH and firing angle is 90℃.

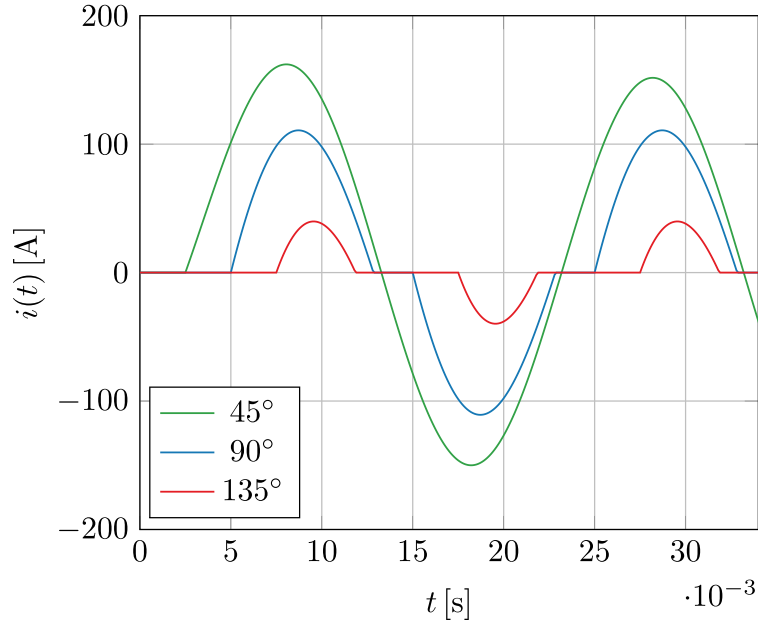**Figure 4.** Current through the RL circuit in Figure 2. Supply voltage is 400 V AC, $R = 1\Omega$, $L = 10\,\text{mH}$ and firing angles were 45°, 90° and 135°.

zero. For large firing angles the current is discontinuous. For firing angles lower than a certain value the current flows continuously and the possibility of regulation becomes significantly lower.

The crest factor is a parameter of a time-dependent function $f(t)$ defined [5] as follows

$$CF = \frac{max(|f(t)|)}{f_{rms}(t)}.$$

Considering a sinusoidal feeding voltage and a firing angle equal to zero, the CF is $\sqrt{2}$ as the resulting current waveform is purely sinusoidal. If the period with zero current alternates, the period with the sinusoidal current CF is $\sqrt{4}$. If two periods with zero current alternate, the period with sinusoidal current CF is $\sqrt{6}$.

CF increases as the firing angle increases. Increasing the firing angle also leads to a lowering of the impulse on a detection particle. For the purpose of this work, the impulse should be constant. CF can be controlled by skipping periods and adjusting the firing angle to maintain a constant impulse. By skipping more periods, large values of CF can be reached.

In real experiments, current waveforms are influenced by the nonlinear character of coil cores and nonlinear tested material. These effects can be easily compensated for by experimentally adjusting the firing angles.

4. Experiment

MPI is a sensitive process and the quality of indications depends on many factors:

- magnetic field distribution, intensity and duration
- magnetic properties of the tested material
- shape of the defect and subsequent leakage field
- properties of detection particles and the method of application
- intensity and spectral characteristics of UV light.

To achieve repeatable results the conditions need to be standardised. Determining the impact of CF on quality of indication requires the influence of all other factors to be minimised by keeping the factors unchanged. The unchanged factors during the experiment are as follows: temperature, diameter, concentration and type of detection particles, method of application of detection particles, magnetisation time, UV light parameters and the process of image taking. The results are independent of the test sample shape if the generated tangential magnetic field is controlled at the evaluation point. If only small changes across the sample are considered, then the calculations of impulse are valid in the neighbourhood of the measurement point (the area of a QQI gauge). A simple symmetrical geometry was chosen to provide for easy magnetic field control. In this section, the experimental setup and methods of evaluation are described.

A sample used for the experiment is shown in Figure 5 and features a standard gauge QQI CX-430 [6] glued onto a block of steel ($10 \times 4 \times 2 cm$).

The supply voltage (400 V, 50 Hz) was controlled by thyristors, as described in the previous section. A pair of coils with electrical steel cores was connected in parallel. The experimental sample was fixed between the cores in a plastic holder tilted at $45°$. This set-up is shown in Figure 6 where the direction of generated magnetic field H_x is along the x axis perpendicular to the vertical defect on QQI. This orientation is described by angles $\beta = 0°$ and $\beta = 180°$ (see Figure 1). Due to the symmetry of the defect and subsequent symmetry of the leakage field $|\mathbf{J}(0°)|/k = |\mathbf{J}(180°)|/k$.

Magnetisation time was set to 8 s, and the time of application of detection particles was 0.4 s. The application of particles started at the same time as the magnetisation as shown in Figure 7. The 8 s interval is long enough for almost all applied particles to flow down. If the application time were longer (by increasing the number of applied particles) or the magnetisation time shorter, the indication created could be washed away when the magnetic force was not present.

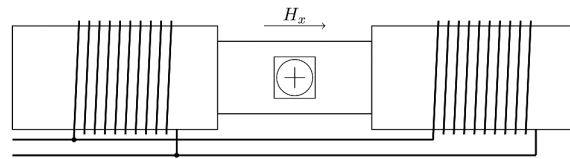**Figure 5.** Steel sample with a QQI.

Figure 6. Schematic of the magnetisation coils with electrical steel cores and the test sample with a QQI gauge.
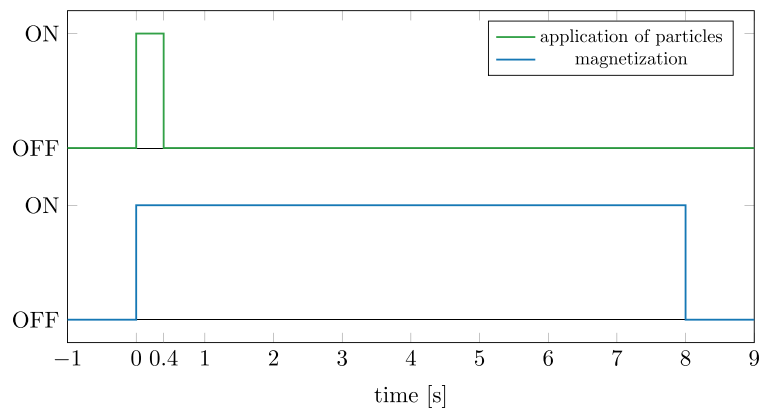

Figure 7. Application of magnetic particles and magnetisation time.

Detection particles were applied from a spray can controlled by a pneumatic valve to deliver the same amount of particles at every repetition. The length of the pneumatic valve activated spray was 0.4 s, which was long enough to spray enough particles on the experimental specimen to generate a clearly visible indication (when the magnetic field was strong enough). Fluorescent magnetic ink *Lumor J*, with mean particle size 5*μ*m, was used. After every repetition, the indication was removed by the solvent cleaner *Overcheck remover*.

Images of indications were captured by a *Canon EOS 650D* under UV light emitted by an LED lamp (peak wavelength 365 nm). Exposure time, ISO and the aperture were set manually (1 s, F26, 400). The intensity of UV light was measured by an *AccuMax XRP-3000* digital UV light metre. UV light intensity was 58 mW/cm^2.

Images have been evaluated visually by a Level 3 certified MPI engineer. To complement this subjective evaluation with an objective one, a method previously used and published by other researchers has been used. The metric used for the evaluation of indication quality is described in detail in [7]. Metric average $\bar{G}$ is defined as follows

$$\bar{G} = \frac{\sum_{i=1}^{n} G_i}{n},$$

where G_i is the value of the green channel of the i-th pixel in the selected area and n is the total number of pixels in the area. The evaluated area was selected manually as a rectangle encompassing the vertical straight indication on a QQI. Two slightly different rectangles were chosen to observe the effect of a different number of pixels. The rectangles measured 550 × 40 pixels and 530 × 30 pixels. The calculation of $\bar{G}$ was performed using two formats: JPEG and CR2. JPEG is a lossy image format with a colour depth of 8-bits per channel, therefore the range of the results calculated from JPEG is from 0 to 255. The *Opencv-python* library was used to read and process the JPEG images. CR2 is a lossless RAW image format developed by *Canon*. The *rawpy* library was used to load CR2. The native resolution of camera ADC is 14-bits, but the image was converted and scaled up to 16-bits by a *rawpy* library, which was used to load and process the images in CR2 format. The results calculated from the CR2 images are in the range of 0 to 65535.

The magnetic field was measured by hall probes at the surface of the tested material. An analog output signal from the hall probe was sampled at 10 kHz by a microcontroller. Samples were transferred to a PC via USB and saved. The instrumentation had been calibrated in a Helmholtz coil before the measurement was performed. The value of $|\mathbf{J}|/k$ was $40 \cdot 10^6 \, \text{sA}^2/\text{m}^2$.

5. Results

Table 1 summarises the values of the green channel as a function of CF and different parameters of image processing. The data from Table 1 are illustrated in Figure 9. There is a certain variation but no trend can be identified. The images of indications are shown in Figure 10. There are no discernible differences in the quality of indications visible to the naked eye. Table 2 shows the standard deviations of average green for different parameters of image processing. The standard deviation of the average calculated from the JPEG format is less than 2 % of the total range, and the standard deviation from CR2 is two times smaller (Figure 8).

Table 1. The average level of the green channel of indications generated by magnetic field waveforms with different CF.

Periods with magnetization	2	2	2	2	2	2
Periods without magnetization	0	2	4	6	8	10
Crest factor [-]	2.55	3.48	4.06	4.52	4.95	5.30
Firing angle [°]	27.7	32.4	34.2	36.4	38.5	40.0
$\bar{G}$ (550 × 40, 8-bits, JPEG) [-]	154.7	144.2	148.2	151.5	156.9	152.8
$\bar{G}$ (530 × 30, 8-bits, JPEG) [-]	168.8	155.8	160.4	164.1	167.7	163.5
$\bar{G}$ (550 × 40, 16-bits, CR2) [-]	52219	51979	52134	52720	53920	52673
$\bar{G}$ (530 × 30, 16-bits, CR2) [-]	55338	54473	54568	55323	56093	55257

Table 2. Standard deviations of evaluated average green levels at the indication and percentage of standard deviations of the total range.

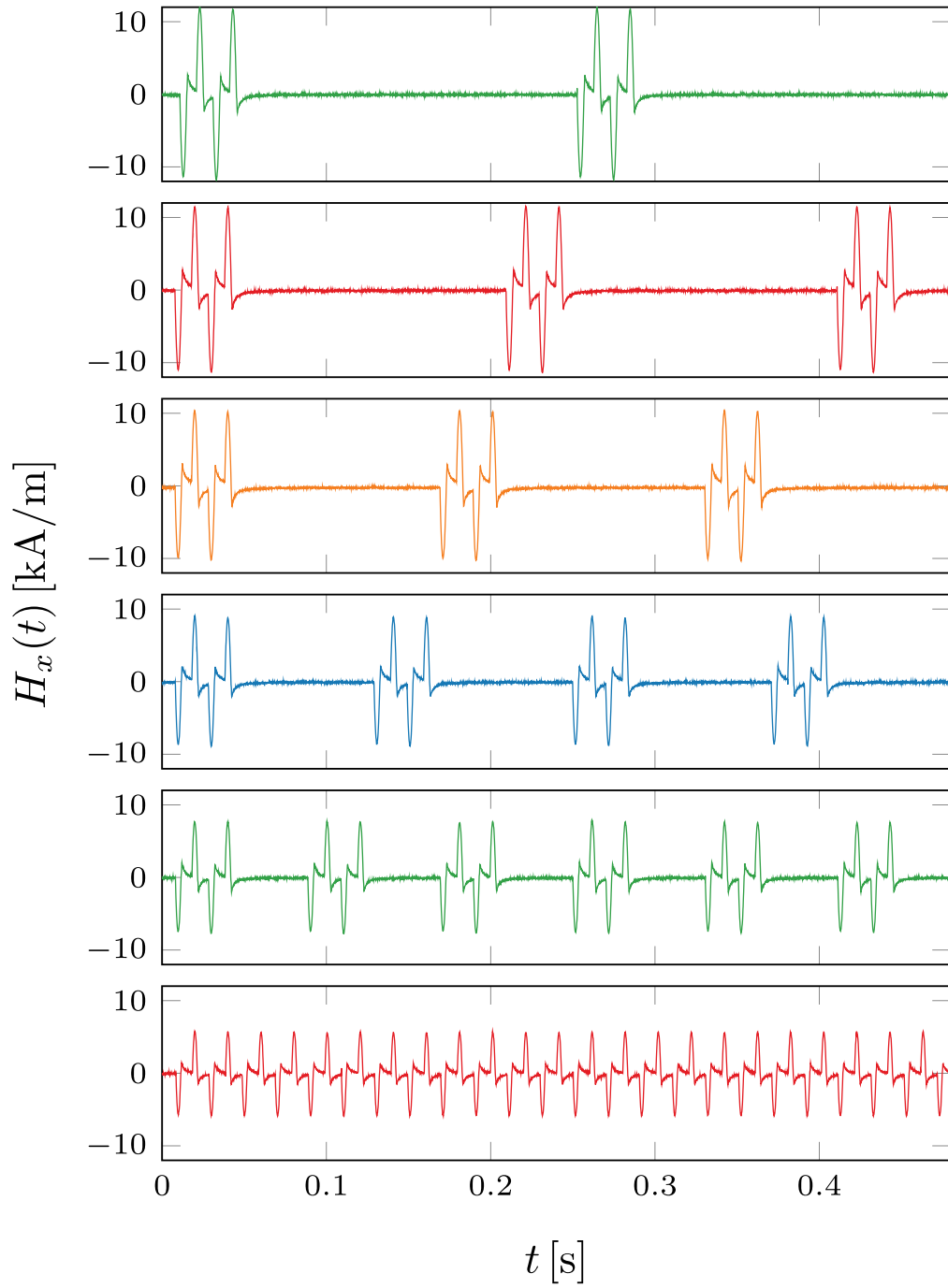|	standard deviation [-]	percentage of range [%]
$\bar{G}$ (550 × 40, 8-bits, JPEG)	4.6	1.8
$\bar{G}$ (530 × 30, 8-bits, JPEG)	4.8	1.9
$\bar{G}$ (550 × 40, 16-bits, CR2)	708	1.1
$\bar{G}$ (530 × 30, 16-bits, CR2)	593	0.9

Figure 8. Magnetic fields generated by a thyristor controlled current. CF is regulated by skipping periods while impulse $|\mathsf{J}|/k$ is kept constant by adjusting the firing angle.
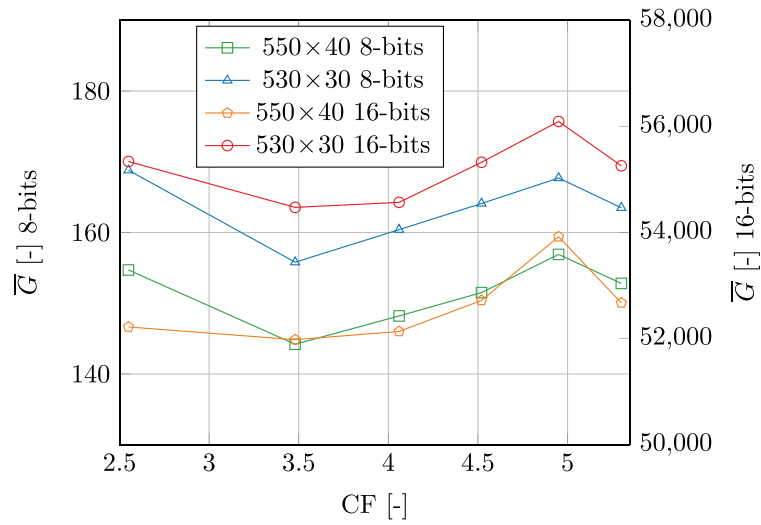
Figure 9. Average green $\bar{G}$ as a function of CF for different sizes of rectangles encompassing the indication and different figure formats.

(a) $CF = 2.55$ (b) $CF = 3.48$ (c) $CF = 4.06$

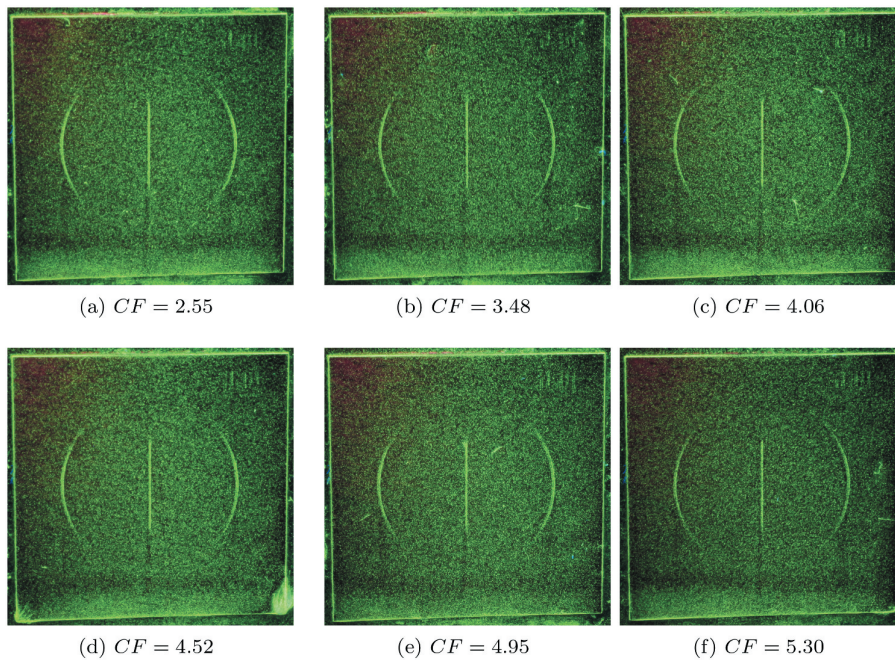(d) $CF = 4.52$ (e) $CF = 4.95$ (f) $CF = 5.30$

Figure 10. Indications generated by magnetic field with the same impulse, but with different crest factors.

If the values of impulse are maintained (as well as the other factors), then the values of $\bar{G}$ are also constant. Constant $\bar{G}$ values imply that the same amount of detection particles have gathered above the defect and the quality of indication is the same. The suggestion to control CF itself does not guarantee a higher quality of indications.

6. Conclusion

Particle behaviour during an MPI process has been experimentally investigated and the results support the theoretical expectations. As for magnetisation, the impulse has been proven as the main factor affecting indication formation in an MPI process. The role of the crest factor is negligible (if there is any at all). This has been explained by theory and confirmed experimentally. The demand in ISO 9934-1 does not seem to be fully grounded. The impulse is the most important factor to be carefully controlled.

ORCID

Pavel Staněk http://orcid.org/0000-0002-6922-0461
Zbyněk Škvor http://orcid.org/0000-0001-6943-784X

References

[1] International Organization for Standardization. Non-destructive testing - magnetic particle testing - part 1: general principles. ISO 9934-1:2015(E) ed. Vernier (Geneva): International Organization for Standardization; 2015.
[2] Staněk P, Škvor Z. Automated magnetic field evaluation for magnetic particle inspection by impulse. J Nondestr Eval. 2019;38(3). DOI:10.1007/s10921-019-0615-4
[3] Hellier C. Handbook of nondestructive evaluation. 1325 Avenue of the Americas New York City USA: McGraw-Hill Professional; 2003.
[4] IAEA Training Course. Liquid penetrant and magnetic particle testing at level 2. 2000.
[5] Radatz J. The IEEE standard dictionary of electrical and electronics terms. IEEE Standards Office; 1997.
[6] American Society for Testing and Materials. Standard guide for magnetic particle testing. ASTM E709-15 ed. West Conshohocken (Pennsylvania): American Society for Testing Materials; 2015.
[7] Lau SMY, Eisenmann D, Peters FE. Development of an image analysis protocol to define noise in wet magnetic particle inspection. Int J Metalcast. 2021;15(4):1317–1325. doi:10.1007/s40962-020-00566-4.

Time Multiplexing of Currents for Magnetic Particle Inspection

Pavel Staněk & Zbyněk Škvor

Published online: 25 Oct 2022.

Submit your article to this journal ⬚

View related articles ⬚

View Crossmark data ⬚

Taylor & Francis
Taylor & Francis Group

Check for updates

Time Multiplexing of Currents for Magnetic Particle Inspection

Pavel Staněk (ID) and Zbyněk Škvor (ID)

Faculty of Electrical Engineering, Department of Electromagnetic Field, Czech Technical University in Prague, Praha, Czech Republic

ABSTRACT

This article concerns magnetization methods for detecting arbitrary oriented defects by magnetic particle inspection. The authors propose a new method of magnetization with omnidirectional detection ability requiring only a single-channel DC or AC power supply. The detection of all defects by the new method can be achieved during a single testing (spraying) cycle.

1. Introduction

Magnetic particle inspection (MPI) is a nondestructive testing (NDT) method that can be used for surface or subsurface defects detection in ferromagnetic materials. MPI is based on the magnetic flux leakage method and a follow-up visual inspection.

The detection ability of MPI is maximal when the magnetic field is perpendicular to the defect, because the strongest leakage field is produced [1,2], but the orientation of the defect is generally unknown. Several approaches to magnetic field generation are used to detect defects of all orientations. Nevertheless, recent advances in solid-state switches, as well as computer control, may allow for new methods.

There are two commonly used methods for arbitrary oriented defects detection. The first method is to perform two full MPI cycles with the first step being the magnetization of the tested material, usually by a yoke or by prod electrodes in a certain direction, followed by the remaining steps of MPI. To detect all defects, a second placement of a yoke or prods, rotated by 90° from the first placement, is necessary [1,2,] followed again by the remaining steps of MPI. Either an AC or DC current can be used. An alternative to this is to rotate the sample under test by 90°. Permanent magnets can also be used with some limitations [2–4].

A second possible approach, known as multidirectional magnetization, is described in [1] . Multidirectional magnetization can be achieved by several

CONTACT Pavel Staněk ✉ stanepa2@fel.cvut.cz 🖥 Faculty of Electrical Engineering, Department of Electromagnetic Field, Czech Technical University in Prague, Technická 2, Praha, 160 00 Prague, Czech Republic

methods, such as the simultaneous combination of different magnetization methods and currents: a combination of DC and AC magnetization, or, a combination of two AC magnetizations. A complex example of how to perform multidirectional magnetization generating rotating magnetic field using multiple coils is studied in [5]. The presented solution consists of many coils positioned around the circle powered by three-phase voltage.

Multidirectional magnetization uses a field that changes its direction during the magnetization phase. This approach, until now, was based on the intuitive assumption that once the magnetic field flux density vector scans all directions, it becomes perpendicular to any defect at a certain time making it likely that the defect will be detected. However, the defect can be detected even when the angle between the defect and the magnetic field vector is not 90°. A detection method using two MPI cycles to detect arbitrary oriented defects illustrates this. The angle is usually considered to be at least 45° [3](5.14) [6].

This article suggests new magnetization scenarios. This is enabled by the quantitative analysis of the magnetic force driving detection particles to form an indication. The analysis, based on the evaluation method published in [7] and used in [8], is carried out for state-of-the-art methods as well as for the new one. The suggested new method based on time-multiplexing of magnetization currents has omnidirectional detection capability while the test bench unit is supplied by single AC phase only. This arrangement is expected to be used in the portable MPI test bench unit design.

2. Theoretical Background

The major part of the development process of MPI test bench units is to design a magnetization circuitry so that the magnetic field results in omnidirectional detection ability. The defect detection ability of a particular MPI process is a quality criteria for the evaluation of a magnetic field generated by the designed circuitry. There are several standard methods on how to evaluate the perfomance of MPI test bench units detection ability of the magnetic field for MPI, including approaches such as pie gauges, QQI shims, or ketos test rings [4,9,10]. The mentioned methods are slow and require all the steps of MPI to be performed. In this article the evaluation method published in [7] is used. The evaluation method is based on magnetic field measurement and therefore can provide real-time feedback for the reconfiguration of magnetization circuitry or current sources settings during the process of optimization of test bench units. In this section, the evaluation method is briefly summarized.

The key quantity responsible for indication forming is the magnetic force driving detection particles toward the defect. The cumulative force effect on a detection particle can be quantified by the impulse of this magnetic force.

The calculation of the impulse is described in [7]. The impulse evaluation method is based on the measurement of components of the magnetic field in the plane tangential to the tested surface. After the time-dependent field components are known, the impulse is calculated as

$$|\mathbf{J}(\beta)| = \int_{t_0}^{t_0+T} kH_0^2(t)\mathrm{dt} = k\int_{t_0}^{t_0+T} (\mathbf{H}(t) \cdot \mathbf{n})^2 \mathrm{dt}, \tag{1}$$

where $|\mathbf{J}(\beta)|$ is the impulse in the direction of $\mathbf{n}$, $\mathbf{n}$ is the unity vector perpendicular to a defect, β is the angle between unity vector $\mathbf{n}$ and the x axis, $\mathbf{H}(H_x(t), H_z(t))$ is the magnetic field vector in a xz plane tangential to the material surface, H_0 is the length of the projection of $\mathbf{H}(t)$ onto the direction of $\mathbf{n}$, and T is magnetization time. The force on a detection particle in a leakage field is a complex function of defect shape and the subsequent leakage field, the position of a particle in the leakage field, the radius of the particle and the permeability of the particle. In equation 1 it is represented by function k which is, generally, unknown. If the MPI is performed under the same conditions (except for magnetic field intensity), k becomes a multiplicative constant. Therefore, normalized impulse $|\mathbf{J}|/k$ is used for the evaluation of the magnetic field.

Components of the magnetic field are measured at a certain point on the surface of a tested material, and therefore, the evaluation process is valid only at the point of measurement or in the neighborhood of the point. If a magnetic field in a larger region should be evaluated, then multiple measurement points must be defined within the region and the evaluation must be performed at all points.

3. Magnetic Field Polarization and Impulse

Let us consider two current loops generating a magnetic field. The vector of the magnetic field in a plane tangential to the surface under test is

$$\mathbf{H} = (H_x(t), H_z(t)) = (H_{x1}(t) + H_{x2}(t), H_{z1}(t) + H_{z2}(t)), \tag{2}$$

where $H_{x1}(t)$ and $H_{x2}(t)$ are x components of magnetic field generated by first and second current loop, respectively, and $H_{z1}(t)$ and $H_{z2}(t)$ are z components of magnetic field generated by first and second current loop, respectively. Unity vector in a plane tangential to the tested surface perpendicular to the defect is $\mathbf{n} = (\cos(\beta), \sin(\beta))$. Let's plug the $\mathbf{H}$ and $\mathbf{n}$ into equation 1:

$$
\begin{aligned}
\frac{|\mathbf{J}(\beta)|}{k} &= \int_0^T (\cos(\beta)H_x(t) + \sin(\beta)H_z(t))^2 dt = \\
&= \cos^2(\beta)\int_0^T H_{x1}^2 + \underline{2H_{x1}H_{x2}} + H_{x2}^2 dt - \\
&\quad - \cos^2(\beta)\int_0^T H_{z1}^2 + \underline{2H_{z1}H_{z2}} + H_{z2}^2 dt + \\
&\quad + \sin(2\beta)\int_0^T H_{x1}H_{z1} + \underline{H_{x1}H_{z2}} + \underline{H_{x2}H_{z1}} + \underline{H_{x2}H_{z2}})dt + \\
&\quad + \int_0^T H_{z1}^2 + \underline{2H_{z1}H_{z2}} + H_{z2}^2 dt,
\end{aligned}
\tag{3}
$$

where T is the magnetization period. The underlined terms vanish when the currents in loops are multiplexed (e.g., never flow simultaneously). This makes time-multiplexed feeding circuits design and control easier when compared to classical sinusoidal current feeding.

The circular polarization of a magnetic field is ideal for arbitrary oriented defects detection as it provides a uniform impulse magnitude in all directions (omnidirectional impulse). Such a polarization may be achieved by two or more sources of a sinusoidal magnetic field with proper phase shifts. It will be shown that there are more possibilities of omnidirectional impulse generation better suited for switched sources.

Figure 1 shows special cases of magnetic field. The magnetic field components are generated by two current loops and the contribution of the first loop only relates to component H_x and the second loop only relates to component H_z. While not a general case, it is a convenient situation to explain. The magnetic field vector is

$$
\mathbf{H} = (H_x(t), H_z(t)) = (H_{x1}(t), H_{z2}(t)),
\tag{4}
$$

and equation 3 reduces to

$$
\begin{aligned}
\frac{|\mathbf{J}(\beta)|}{k} &= \int_0^T (\cos(\beta)H_x(t) + \sin(\beta)H_z(t))^2 dt = \\
&= \cos^2(\beta)\int_0^T H_{x1}^2 dt - \cos^2(\beta)\int_0^T H_{z2}^2 dt + \\
&\quad + \sin(2\beta)\int_0^T \underline{H_{x1}H_{z2}} dt + \int_0^T H_{z2}^2 dt.
\end{aligned}
\tag{5}
$$

When using time-multiplexing, the underlined term again vanishes. The value of integrals in remaining terms are independent of the phase of the AC supply; therefore, the omnidirectional detection ability can be achieved by single phase supply.

There are four triplets of figures (each row) in Figure 1 showing the components of a magnetic field, corresponding polarization, and finally,
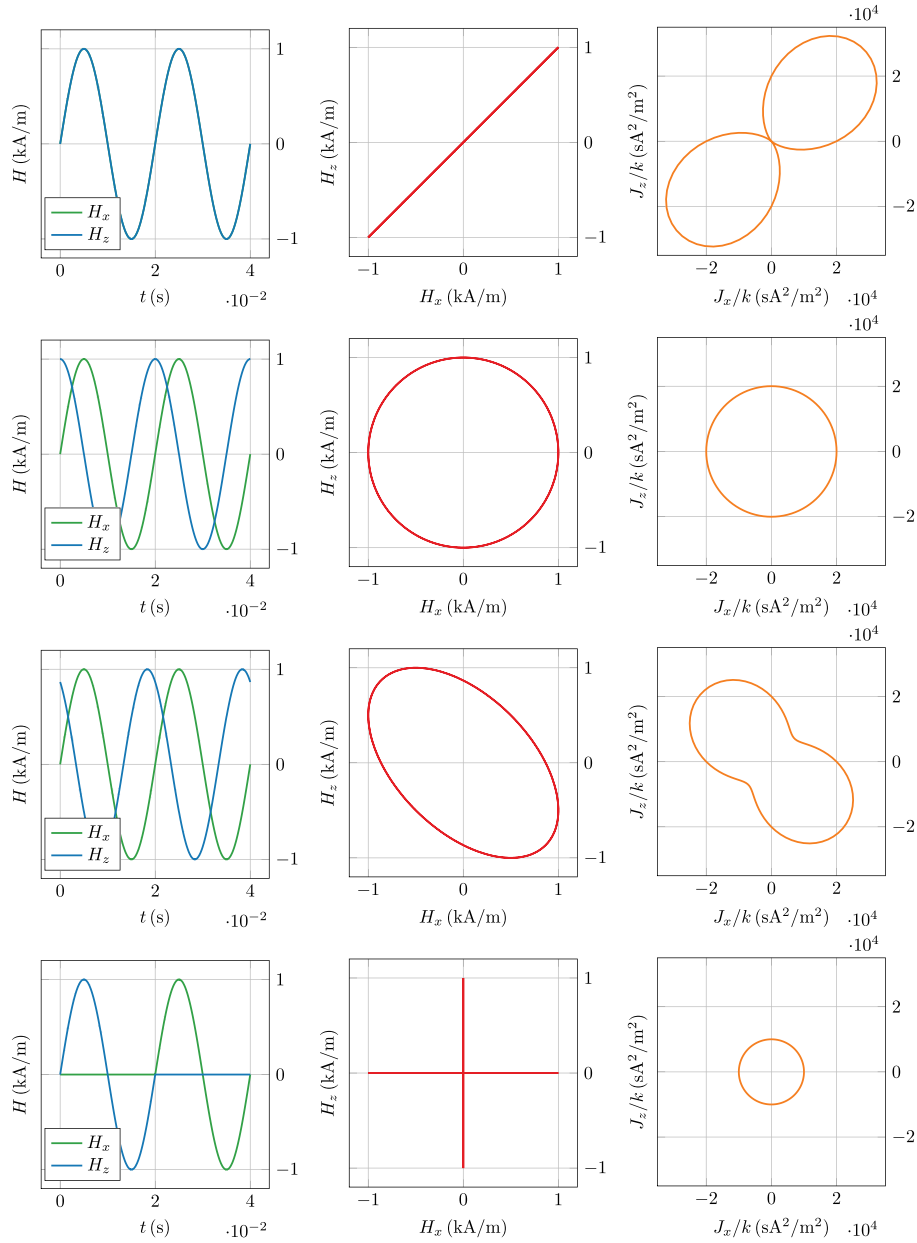
Figure 1. Magnetic field components, polarizations and impulses. The first column contains time dependant waveforms of magnetic field components on the tested surface. The second column contains the corresponding polarization of the magnetic field components in the first column. Last column shows normalized impulse of the magnetic force on the detection particle. The first three rows show situations of simultaneous current flow through both loops. The sinusoidal components of magnetic field have different phase shift and therefore different force impulse on the detection particles. In the last row, the magnetic field components are time-multiplexed, still resulting in omnidirectional detection ability.

impulse. The impulse patterns in the last column are solutions of equation 5. For the sake of simplicity, the magnetic field components are zero, or sinusoidal with a different phase shift, but featuring the same magnitude.

The first row shows the situation of both current loops powered by the same voltage (same phase). If currents in both loops are flowing simultaneously, polarization is linear and some defects will not be detected. Blind angles (i.e., cracks under these angles not likely to be detected) are shown in the third figure where the zero impulse, in a direction perpendicular to linear polarization, can be seen. The second row demonstrates an ideal case of magnetic field components having a 90° phase shift. The impulse pattern is omnidirectional (circular). The third row illustrates the situation of a 120° phase shift, which is readily available from a three-phase power grid and, therefore, commonly used. The impulse pattern is not ideal, but there is nonzero impulse in all directions. If the minimum impulse is above a detection threshold, all defects will likely be detected. The last row shows a novel approach using time multiplexing. One period of the sinusoidal magnetic field alternates with another period of a zero magnetic field. The waveforms of H_x and H_z are shifted by one period. The resulting polarization is cross-shaped; nevertheless. the impulse pattern is again circular, e.g., providing an ideal omnidirectional detection ability (only the diameter is halved when compared to the impulse pattern in the second row). If the time duration were doubled, the impulse patterns would have the same diameter as the pattern in the first row.

The time multiplexing method enables the detection of all defects using two current loops powered by a single phase AC or DC voltage. In the case of simultaneous current flow in both loops, polarization will be linear, and therefore, the impulse pattern will suffer from blind angles. When the currents are time multiplexed between the loops, the polarization consists of two lines under 90° generating a circular impulse pattern with no blind angles. This case is shown in the last row of Figure 1.

The time-multiplexing approach can be used for magnetic field optimization or synthesis. The advantage of the time-multiplexing method lies in it having no effect of the mutual coupling of current loops and has the possibility of using only a single-channel power supply (AC or DC). In the case of temperature dependency and thyristor regulation, the current can be maintained by changing the firing angle with no change in the resulting impulse. Another benefit is that the impulse always increases in a certain direction if the root-mean-square value of the current increases. If multiplexing is not used and the current is flowing in multiple loops simultaneously, the value of the impulse can decrease even if the total root-mean-square value of the current increases. The advantage of time-multiplexing over a two-step MPI is that the impulse may be balanced in all directions when using multiplexing, whereas using a two-step MPI never balances the impulse and has a maximum in the direction of the maximal field. A disadvantage is that the multiplexing

approach is potentially slower, but this can be compensated by increasing the current. There is also a slightly higher demand on regulation hardware and software, but commonly used hardware can usually be reprogrammed for a time multiplex. Time multiplexing also simplifies the design of test bench units. If the classical approach of simultaneous current flow is used, the induced voltages (as a result of the mutual coupling of current loops) brings the optimization or synthesis of a magnetic field additional degrees of freedom.

In a real situation, both current loops would probably contribute to both components of the magnetic field. The synthesis or optimization goal is to achieve an omnidirectional impulse. The requirement for an omnidirectional impulse pattern is to use at least two current loops generating magnetic fields of different directions (direct or indirect magnetization). Complex parts to be tested by MPI may require more current loops.

4. Experiment

An experiment was performed to support theoretical findings. The goal was to prove that the time-multiplexing magnetization method using only one phase supply is capable of detecting arbitrary oriented defect. Standard QQI gauge CX-430 [2] with circular and cross-shaped defect was glued onto a block of steel.

Three rounds of MPI were performed. The test steel block with gauge was magnetized by two different current loops using commercially available test bench unit. In the first round, two phases with mutual phase shift 120° were used for magnetization; e.i., the classical multidirectional approach was used. Current was flowing simultaneously in both loops for 5 s. In the second round, two phases with the same phase shift as before were used for magnetization, but the current was multiplexed every 0.5 s. The duration of the magnetization was 10 s. In the third round, only one phase was used to supply both current loops. The multiplex period was again 0.5 s and the duration of magnetization was 10 s. The current was controlled by thyristors in all cases, and the same firing angles were used for all three runs. The waveforms inFigure 3 show the periods of zero and non-zero currents during the performed magnetizations.

Images of indications taken under UV light are shown in Figure 2. The results in Figure 2 show that all the magnetization methods can be successfully used to detect defects of all orientations.

5. Conclusion

A method of generating a magnetic field enabling the detection of arbitrary oriented defects using a single power source with time multiplexing has been presented and compared to other commonly used magnetization methods. The theoretical findings were supported by the experiment. The suggested

(a) classical multidirectional magnetization: two current sources

(b) time-multiplexing: two current sources

(c) time-multiplexing: one current source

Figure 2. Indications generated by different magnetization methods. These indications show that omnidirectional detection ability has been achieved by the new magnetization method. The quality of indications generated by all methods is fully comparable.

time [s]
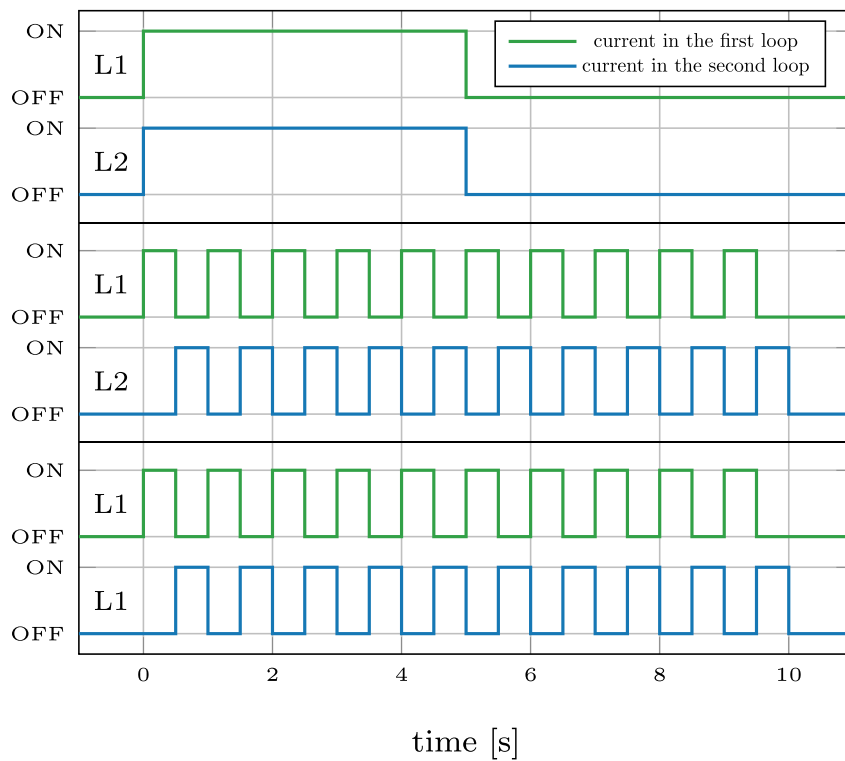
Figure 3. ON/OFF periods of thyristors controlling current flowing through magnetization loops during the experiment. There are two waveforms (green and blue) for each MPI cycle. L1 and L2 indicates the phases used to supply current loops. European standard (230V,50Hz) three phase supply (L1, L2, L3, N, PE) was used [11].

method of magnetic field generation can be used for arbitrary oriented defects detection and may simplify instrumentation without compromising crack detection. This method also reduces the complexity of the optimization or synthesis of a magnetic field used for testing.

Disclosure Statement

No potential conflict of interest was reported by the author(s).

ORCID

Pavel Staněk 🔘 http://orcid.org/0000-0002-6922-0461
Zbyněk Škvor 🔘 http://orcid.org/0000-0001-6943-784X

References

1. J. Thomas Schmidt, K. Skeie, and P. McIntire, *Nondestructive Testing Handbook: Magnetic Particle Testing*, 1711 Arlingate Lane Columbus, OH 43228-0518 USA: American Society for Nondestructive Testing, (1989).
2. ASTM, *Standard Guide for Magnetic Particle Testing E709-15*, 100 Barr Harbor Drive, Conshohocken, PA 19428 United States: Standard, American Society for Testing and Materials, (2015).
3. C. Hellier, *Handbook of Nondestructive Evaluation*, 1325 Avenue of the Americas, New York NY 10019, United States: McGraw-Hill Professional, (2003).
4. IAEA Training Course Series, *Liquid Penetrant and Magnetic Particle Testing at Level 2* (Wagramer Strasse 5, A-1400 Vienna, Austria: International Atomic Energy Agency) (2000).
5. K. Fukuoka et al., *Electr. Eng. Japan* **204** (4), 36–42 (2018). DOI: 10.1002/eej.23109.
6. F. C. Campbell, *Inspection of Metals: Understanding the Basics*, 9639 Kinsman Road Materials Park, OH 44073-0002, United States: ASM International, (2013).
7. P. Staněk and Z. Škvor, *J. Nondestr. Eval.* **38** (3) (2019). Doi: 10.1007/s10921-019-0615-4.
8. P. Staněk and Z. Škvor, *Nondestruct. Test. Eval.* () (2022). Doi: 10.1080/10589759.2022. 2066663.
9. D. Eisenmann et al., Fundamental engineering studies of magnetic particle inspection and impact on standards and industrial practice. (2014).

10. P. E. Mix, *Introduction to Nondestructive Testing: A Training Guide*, 111 River Street Hoboken, NJ 07030, United State: John Wiley & Sons, (2005).

11. IEC, *IEC 60445 Basic and Safety Principles for man-machine Interface, Marking and Identification – Identification of Equipment Terminals, Conductor Terminations and Conductors*, rue de Varembé 3, 1211 Genève 20, Switzerland: International Electrotechnical Commission, (2021).